PCCP

Nanoparticles in Ionic Liquids: Interactions and Organization

Journal:	*Physical Chemistry Chemical Physics*
Manuscript ID:	CP-PER-03-2015-001620.R1
Article Type:	Perspective
Date Submitted by the Author:	09-Jun-2015

Complete List of Authors:	He, Zhiqi; University at Buffalo - The State University of New York, Dept of Chemical & Biological Engineering Alexandridis, Paschalis; University at Buffalo - The State University of New York, Dept of Chemical & Biological Engineering

Cite this: DOI: 10.1039/c0xx00000x

www.rsc.org/xxxxxx

PERSPECTIVE

Nanoparticles in ionic liquids: Interactions and organization

Zhiqi He[a] and Paschalis Alexandridis*[a]

Received (in XXX, XXX) Xth XXXXXXXXX 20XX, Accepted Xth XXXXXXXXX 20XX
DOI: 10.1039/b000000x

Ionic liquids (ILs), defined as low-melting organic salts, are a novel class of compounds with unique properties and a combinatorially great chemical diversity. Ionic liquids are utilized as synthesis and dispersion media for nanoparticles as well as for surface functionalization. Ionic liquid and nanoparticle hybrid systems are governed by a combined effect of several intermolecular interactions between their constituents. For each interaction, including van der Waals, electrostatic, structural, solvophobic, steric, and hydrogen bonding, the characterization and quantitative calculation methods together with factors affecting these interactions are reviewed here. Various self-organized structures based on nanoparticles in ionic liquids are generated as a result of a balance of these intermolecular interactions. These structures, including colloidal glasses and gels, lyotropic liquid crystals, nanoparticle-stabilized ionic liquid-containing emulsions, ionic liquid surface-functionalized nanoparticles, and nanoscale ionic materials, possess properties of both ionic liquids and nanoparticles, which render them useful as novel materials especially in electrochemical and catalysis applications. This review of the interactions within nanoparticle dispersions in ionic liquids and of the structure of nanoparticle and ionic liquid hybrids provides guidance on the rational design of novel ionic liquid-based materials, enabling applications in broad areas.

1. Introduction

Ionic liquids (ILs) are molten salts typically consisting of organic cations and organic or inorganic anions. The term "ionic liquids" initially defined low-melting salts[1], but in more recent literature,[2, 3] "ionic liquids" refers to molten salts with melting point below 100 °C, often specified as Room Temperature Ionic Liquids (RTILs).[4]

Ethylammonium nitrate (EAN, $(C_2H_5)NH_3^+ \cdot NO_3^-$) is believed to be the first reported room temperature ionic liquid.[5] The discovery in the 1990s of ionic liquids that are stable (at least at room temperature) towards hydrolysis, e.g., tetrafluoroborate, hexafluorophosphate, nitrate, sulfate and acetate salts, spurred significant research efforts.[6, 7] Ionic liquids offer many advantages such as negligible vapor pressure, good thermal and chemical stability, high ionic conductivity, broad electrochemical potential windows, good solubility and high synthetic flexibility.[4, 8-10] Ionic liquids have been called "designer solvents" for the opportunities they afford in the rational design of the cation and the anion chemical structures through proper consideration of structure-function relationships.[11-16] Ionic liquid solvents are used for extraction and separations in analytical chemistry.[17-19] The unique properties of ionic liquids also motivate their applications as electrolytes in lithium batteries[20, 21] and in dye-sensitized solar cells[22], and their consideration as solvents for drug delivery[23] and biomass processing[24-26]. Commonly used cations and anions of ionic liquids are presented in Figure 1.

Ionic liquids are not simple liquids. Their ions are generally asymmetric, with delocalized electrostatic charges.[27] Studies on the physicochemical properties of ionic liquids have shown that the molecular structure of ionic liquids affects their properties, e.g., thermal properties (including melting point, heat capacity, thermal stability), solubility, viscosity, surface tension, diffusivity, and electrical conductivity.[28-32] The molecular forces and interactions of ionic liquids are much more complicated than those of common classical salts.[33]

ILs share some similarities with water. Early research reported a similar formation process of surfactant micelles in ethylammonium nitrate and in water.[34, 35] Water exists as a mixture of free water molecules and hydrogen-bonded water clusters.[36] Correspondingly, ILs appear to be a mixture of free ions and hydrogen-bonded ionic supramolecular structures.[7, 37] The notable characteristics of ILs are primarily attributable to their ionic nature. The combination of the strong Coulombic interactions and weak directional interactions (including hydrogen bonding interactions, cation-π interactions, van der Waals inductive and dispersion interactions) may induce the formation of nano-scale structures in ILs and IL/solvent or IL/solute mixtures.[11]

Imidazolium-based cations consist of a polar head group and a non-polar alkyl side chain. Ionic liquids with an imidazolium cation can form hydrogen-bonded polymeric supramolecular aggregates with the general form of $[Im_xX_{x-n}]^{n+}$ or $[Im_{x-n}X_x]^{n-}$, where Im represents the cation and X represents the anion.[38] For those imidazolium-based ionic liquids with long alkyl side-chains, the alkyl chains can segregate to form nonpolar domains, while other parts of the ionic liquid form polar domains, as shown in

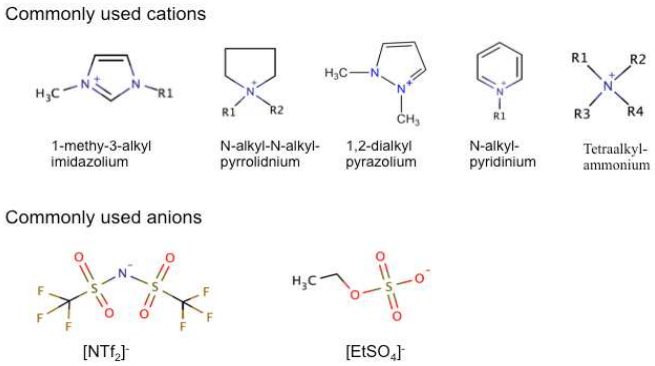

Figure 1. Commonly used cations and anions of ionic liquids (Rn represents alkyl chain).

Figure 2.[39] As the length of alkyl chain increases, the nonpolar domains increase in size and become more connected, leading to a microphase separation such as liquid crystal formation. Anisotropic-like liquids are observed in this case.[40] Such highly hydrogen-bonded networks with polar and nonpolar nanodomains facilitate the dissolution of various substances in ILs.[41, 42] The distribution of solutes in ionic liquids is much different than that in homogeneous solvents because of the existence of structural heterogeneities within ILs.[39] The solutes tend to localize into the nano-scale domains for which they have higher affinity.[43]

Multiple intermolecular interactions assist ionic liquids in dissolving the otherwise insoluble cellulose[44-46]. Ionic liquids are also used as reaction media, playing the role of solvent and template.[47-50] Considering colloidal systems, ionic liquids are explored as dispersoids or dispersion media,[51] facilitating the dispersion of metal nanoparticles[52] , nanostructured inorganic particles[53] and carbon nanotubes[54, 55]. Some colloidal particles can be stably suspended in ionic liquids without the need to add classical stabilizers such as surfactants and/or polymers.[51] Ionic liquids, contributing to electrostatic forces on the surface of nanoparticles, can also be utilized as stabilizers for nanoparticles synthesized in aqueous solution.[56, 57] A comprehensive analysis of nanoparticle dispersion in ionic liquids can therefore provide an improved fundamental understanding needed to support emerging applications of ILs in nanoparticle synthesis, in chemical reactions involving nanoparticles, and in hybrid materials that incorporate ILs and nanoparticles.

In this review we address hybrids comprising ionic liquids and nanoparticles without or with other ingredients such as polymers and amphiphiles. An understanding of structure and dynamics in ionic liquid and nanoparticle hybrid systems can further contribute to the applications of such hybrids in emerging fields like lithium batteries and solar cells. Very recent reviews about ionic liquids have addressed nanostructure of ionic liquids[58], and the use of ionic liquids as media for nanomaterial synthesis[48, 59] or amphiphile self-assembly[58, 60]. However, the stabilization of nanoparticles in ionic liquids on the basis of intermolecular interactions, and the ensuing structure and organization have not been addressed in previous reviews. The stability of nanoparticles in ionic liquids can be viewed from two sides, physical stability and chemical stability. In this review, we focus on physical stability, which macroscopically describes whether a colloidal

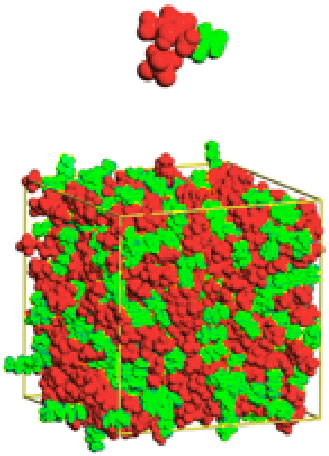

Figure 2. Segregation in domains is visible in liquid-phase molecular dynamics simulations (250 ion pairs of 1-hexyl-3-methylimidazolium hexafluorophosphate [C_6mim][PF_6]). Red (dark) corresponds to the imidazolium ring of the cation (plus some atoms attached to it) and the entire PF_6 anion, and green (light) corresponds the "nonpolar" side chain.[27] Copyright 2007 American Chemical Society.

system maintains a single phase, while microscopically describes whether the nanoparticles agglomerate or aggregate in certain dispersant media.

In what follows, we address the stability of nanoparticle dispersions in ionic liquids and the nanoparticle organization in ionic liquid-nanoparticle hybrid systems. First, we discuss intermolecular interactions acting within dispersions of nanoparticles in ionic liquids. Van der Waals, electrostatic, structural, solvophobic, steric and hydrogen bonding interactions are presented, followed by a combination of the interactions toward maintaining nanoparticle dispersion stability in ionic liquids. Both internal and external factors that affect the interactions mentioned above and consequently impact the nanoparticle stability in ionic liquids are reviewed. Next, self-organized structures based on nanoparticles and ionic liquids, including colloidal glasses and gels, lyotropic liquid crystals, nanoparticle-stabilized ionic liquid-containing emulsions, ionic liquid surface-functionalized nanoparticles and nanoscale ionic materials, are reviewed in the context of the intermolecular interactions that stabilize them.

2. Nanoparticle stabilization in ionic liquids

Metal nanoparticles attract significant attention on the basis of their novel properties.[61, 62] Several publications have reported high-yield synthesis of metallic nanoparticles in ILs.[63-65] In fact, metal nanoparticles synthesized in ionic liquids are reported to be mono-dispersed and non-agglomerated as a result of ionic liquid stabilization.[59, 66-69]

In order to prepare desired nanoparticles in ionic liquids, the stability of the nanoparticle dispersion should be carefully controlled. Any factors affecting the stability of nanoparticles in ionic liquids may lead to nanoparticle size[70-73] and/or morphology[74-78] changes during synthesis. The size and size distribution of nanoparticles synthesized in ionic liquids are affected by physicochemical properties of ionic liquids, which affect the nanoparticle stabilization. For example, smaller

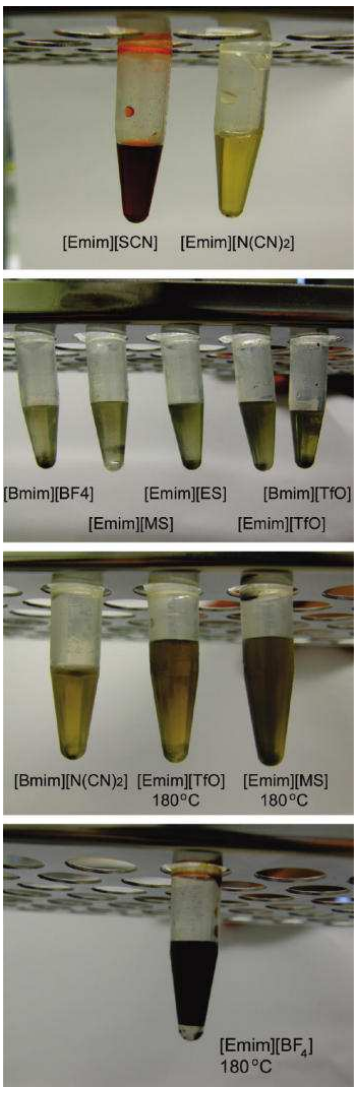

Figure 3. Photographs of Fe_3C nanoparticle dispersions in ILs. The temperature values given for some samples are the temperatures at which the dispersions were prepared. Absence of a temperature value indicates dispersions prepared at room temperature.[79] The ionic liquids used are noted inside the figure: cations are 1-ethyl-3-methylimidazolium $[Emim]^+$ and 1-butyl-3-methylimidazolium $[Bmim]^+$; anions are ethylsulfate $[ES]^-$, methane-sulfonate $[MS]^-$, trifluoromethylsulfonate(triflate) $[TfO]^-$, tetrafluoroborate $[BF_4]^-$, dicyanamide $[N(CN)_2]^-$, and thiocyanate $[SCN]^-$. Copyright 2010 American Chemical Society.

diameter and narrower distributions of synthesized nickel and ZnO nanoparticles were prepared in ionic liquids with longer side chains, because the long side chain impacted the nanoparticle stability in ionic liquids by altering the physicochemical properties of ionic liquid as well as the interactions between ionic liquid and nanoparticle.[66, 75] Larger size or varied morphologies of synthesized nanoparticles can be caused by conglomeration of unstable prime nanoparticles, which may result from smaller ionic liquid anions exhibiting stronger cation-anion Coulomb attraction,[80] or less coordinating anion of ionic liquid,[68, 78] or higher temperature decreasing the viscosity of the ionic liquid and increasing the diffusive velocities of the sputtered nanoparticles[81, 82]. Thus, an improved understanding of the stability of nanoparticle dispersions in ionic liquids will

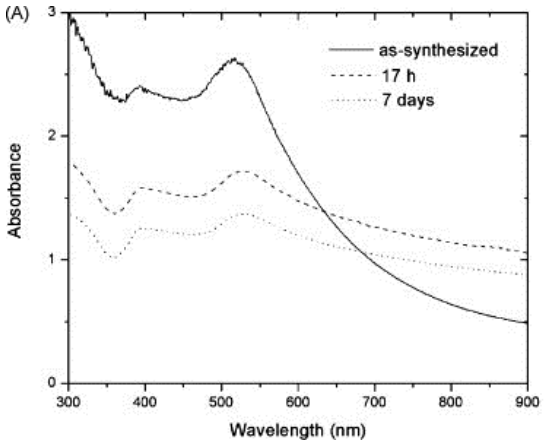

Figure 4. UV–vis spectra of Au nanoparticles synthesized in pure 1-butyl-3-methylimidazolium hexafluorophosphate ([Bmim][PF_6]). A decrease in the intensity of the plasmon band at 530 nm along with an increase in the high wavelength region of the absorption spectra over 17h indicate nanoparticle aggregation. The overall intensity decreased after several days, suggesting that the nanoparticles precipitated.[83, 84] Copyright 2010 Elsevier.

significantly assist efforts directed toward the synthesis of nanoparticles with controlled size and morphology in ionic liquids.

In this section, we review the stability of nanoparticle dispersions in ionic liquids and the intermolecular forces affecting such stability. We first introduce characterization methods of nanoparticle dispersion stability in ionic liquids, followed by several subsections each addressing a specific interaction that can contribute to colloidal stabilization. We start by considering the basic forces in typical colloidal systems, e.g., van der Waals and electrostatic interactions. Then we analyze the interactions of special interest to in ionic liquid-based colloidal systems, e.g., hydrogen bonding and structural forces. Moreover, steric interactions are discussed in the context of added macromolecular stabilizers. Both internal and external factors affecting the interactions mentioned above and consequently impacting on nanoparticle stability in ionic liquids are reviewed in the later part. An overview on the interactions acting in tandem on the ionic liquid and nanoparticle hybrid systems is presented in the last part of this section.

2.1 Characterization of nanoparticle dispersion stability in ionic liquids

There are several ways to assess the dispersion stability of nanoparticles in ionic liquids. In general, colloidal stability is assessed by examination of nanoparticle size distribution over time.[85] The simplest method is visual or spectroscopic inspection, in other words, observing the color and/or sediment of nanoparticle/ionic liquid dispersions.[86] This method is usually applied in metal nanoparticles since they exhibit their specified color at uniform dispersion but show a different color when precipitated. An absorbance peak appears at a certain wavelength when nanoparticles are mono-dispersed, while the absorption wavelength shifts and the baseline increases when aggregates form.[87] For example, mono-dispersed Fe_3C nanoparticles presented a deep orange-red or yellowish color and a transparent solution in compatible ionic liquids, 1-ethyl-3-

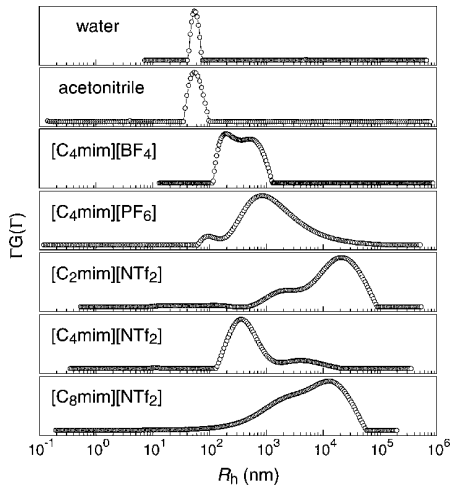

Figure 5. Size distribution curves for bare silica particles (with average radius of 62 nm) in deionized water, acetonitrile, and various ILs measured by DLS at 25 °C. DLS measurements for the IL dispersions were conducted after 12 h of quiet standing of the prepared samples.[88] The ionic liquids tested are: 1-butyl-3-methylimidazolium tetrafluoroborate [Bmim][BF_4], 1-butyl-3-methylimidazolium hexafluorophosphate [Bmim][PF_6], 1-ethyl-3-methylimidazolium bis(trifluoromethylsulfonyl)imide [Emim][NTf_2], 1-butyl-3-methylimidazolium bis(trifluoromethylsulfonyl)imide [Bmim][NTf_2], and 1- octyl-3-methylimidazolium bis(trifluoromethylsulfonyl)imide [C_8mim][NTf_2]. Copyright 2008 American Chemical Society.

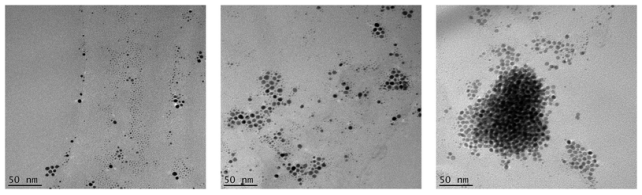

Figure 6. Representative TEM images of gold nanoparticles in the ionic liquid [Bmim[$N(CN)_2$] obtained 2 hours (left), 6 hours (middle) and 24 hours (right) after sputtering. The TEM samples were prepared by dipping a copper grid covered with a lacey carbon film into the ionic liquid containing gold NPs, and by draining the excess of ionic liquid with filter paper.[84] Copyright 2012 the Owner Societies.

methylimidazolium thiocyanate ([Emim][SCN]) and 1-ethyl-3-methyl-imidazolium-dicyanamide ([Emim][$N(CN)_2$]), while non-stable Fe_3C particles resulted in a turbid dispersion with a significant amount of black sediment, as shown in Figure 3.[79] A color change of the nanoparticle/ionic liquid dispersion as a function of time was reported in the case of gold nanoparticles (4-7 nm diameter) synthesized in 1-butyl-3-methylimidazolium ionic liquids. The suspension showed a red color at the time of synthesis, characteristic for gold nanoparticles.[84] The UV–vis spectra of gold nanoparticles exhibit a typical surface plasmon resonance (SPR) band at around 530 nm.[89] After some time the suspension turned purple, and it finally turned out to be lighter colored with black sediment at the bottom of the cuvette, indicating coagulation followed by sedimentation of the nanoparticles.[84] Several studies have considered gold nanoparticle synthesis and dispersion in imidazolium-based and pyrrolidinium-based ionic liquids.[70, 81, 84, 90-95] UV-vis spectra on gold nanoparticle dispersion in 1-butyl-3-methylimidazolium

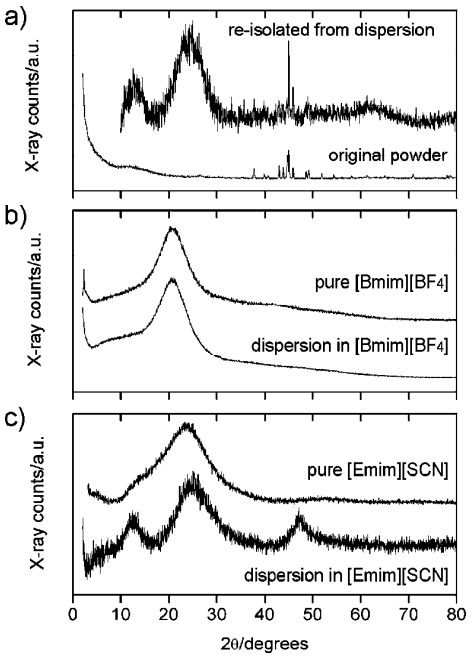

Figure 7. WAXS patterns of Fe_3C powder and its dispersions in ILs: (a) original Fe_3C powder and Fe_3C powder reisolated from [Emim][SCN], (b) pure [Bmim][BF_4] and Fe_3C in [Bmim][BF_4], and (c) pure [Emim][SCN] and Fe_3C in [Emim][SCN].[79] Copyright 2010 American Chemical Society.

hexafluorophosphate ([Bmim][PF_6]) (Figure 4) showed the intensity of the plasmon band to decrease while the overall intensity of the absorption spectra to increase in the large-wavelength region over the 24 hours after synthesis, which indicated the formation of aggregates.[83, 84]

Scattering methods provide ways to assess colloidal stability by providing information on particle size.[79, 88] The radius of nanoparticles dispersed in ionic liquids can be calculated by fitting the scattering intensities obtained by small angle X-ray scattering (SAXS) to an appropriate form factor.[79] Dynamic light scattering (DLS) can quantitatively determine the size distribution of nanoparticle dispersions. Figure 5 shows the size distribution curves for bare silica nanoparticles dispersed in different solvents. For DLS data analysis, two important parameters are needed, the viscosity and dielectric constant of the solvent. Viscosity and dielectric constant values for numerous ionic liquids have been reported together with other physicochemical properties.[8, 96, 97]

Transmission electron microscopy (TEM) and scanning electron microscopy (SEM) both provide direct ways to visualize nanoparticles. Ionic liquids provide the unique advantage of allowing SEM without accumulation of electron charges, thus enabling the observation of nanoparticles wetted with ionic liquids.[98] The nanoparticle dispersion can be imaged by TEM or SEM to observe whether the nanoparticles aggregate.[84, 93] Representative TEM images of gold nanoparticles in the ionic liquid [Bmim][$N(CN)_2$]), obtained at different times after sputtering with a gold foil target, are shown in Figure 6. Electron microscopy provides a good way to compare the size and morphology of nanoparticles synthesized in different solvents or with different methods.[79, 83, 87, 88] However, electron microscopy

requires sample deposition onto support grids or films, which means that the suspension of nanoparticles in the solvent is disturbed at the time of sample preparation.

The methods described above are designed to assess the physical stability of nanoparticle dispersions, reflected by whether and how the nanoparticles aggregate in solvents. However, chemical stability should also be considered. Chemically stable nanoparticles do not react with the solvents they are dispersed in, and retain their properties such as catalytic ability and surface functionality. X-ray scattering has been applied to examine whether there is a chemical reaction taking place by comparing the X-ray patterns of original nanoparticle with nanoparticle isolated from ionic liquids after dispersion (see Figure 7).[79] Powder X-ray diffraction conducted on dispersed LaF_3:Ln^{3+} nanocrystals synthesized in 1-butyl-methylpyrrolidinium bis(trifluoromethanesulfonyl)amide ([Bmpyr][Tf_2N]) or 1-butyl-1-methylpyrrolidinium trifluoromethanesulfonate ([Bmpyr][TfO]) ionic liquids suggested that neither the crystalline structure nor the nanoparticle size changed after the nanocrystal dispersion in the ionic liquid.[99]

In addition to the general methods highlighted above, some nanoparticles have special properties which can be utilized in characterizing their dispersion stability in ionic liquids. For example, the colloidal stability of magnetite nanoparticles in the ionic liquid 1-ethyl-3-methylimidazolium ethylsulfate ([Emim][$EtSO_4$]) has been tested by magnetic sedimentation, centrifugation and redispersion, and by 'in situ' HREM pictures of the dispersions.[100]

2.2 Electrostatic interactions and van der Waals interactions

Electrostatic interactions and van der Waals interactions are present in almost all colloidal systems.[101-103] The van der Waals force, arising from correlations between electrons motions in two neighboring molecules, is a short-range unidirectional force that is relatively weak compared to other inter-molecular interactions.[101] The electrostatic interaction is appreciable for nanoparticles in ionic liquids that consist of cations and anions. In these cases, positively or negatively charged ion clusters, instead of separate single ions, surround the nanoparticle surface to build an electrical double-layer, thus providing a electrostatic force to keep the nanoparticles apart from each other.[104]

The role of electrostatics in stabilizing the nanoparticles synthesized in ionic liquids has been well recognized.[56, 84, 105, 106] The ions or ion clusters are attracted on the nanoparticle surface by electrostatic forces.[69] The ionic liquid cations are attracted to the surface of a negative charged nanoparticle to form a positive ion layer, and then counterions form a second layer on the nanoparticle surface by electrostatic attraction.[93, 107, 108] It has been reported that anionic semiorganized imidazolium supramolecular aggregates $[(Bmim)_{x-n}(PF_6)_x]^{n-}$ formed a first layer surrounding gold nanoparticle (with a diameter of 2.6±0.3 nm), whereas supramolecular cationic aggregates $[(Bmim)_x(PF_6)_{x-n}]^{n+}$ laid adjacent to the first layer to provide charge balance (Figure 8).[109] The electrical double layer efficiently keeps nanoparticles from aggregating. 1-butyl-3-methylimidazolium lauryl sulfate ([Bmim][$C_{12}H_{25}OSO_3$]) was reported to form a double layer structure around synthesized gold nanocrystals to provide electrostatic forces, which stabilized the

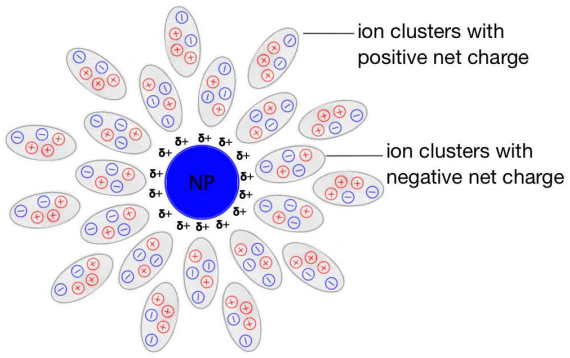

Figure 8. Schematic of ion clusters surrounding nanoparticles. The ion clusters form a protective electrical double layer.

gold nanocrystals together with van der Waals interactions between butyl and lauryl side chains of the ionic liquid that contributed a secondary stabilization.[93] A molecular dynamics simulation of carbon nanotube dispersions in [Emim][TFSI] ionic liquid explored the effects of electrostatic interactions by applying different surface charge densities (-0.5, 0.0, +0.5 [e/nm^2]) on the carbon nanotube.[106] On the surface of a neutral carbon nanotube, $[Emim]^+$ cations tended to lay parallel, while $[TFSI]^-$ anions had the same probability to lay parallel and perpendicular. It turned out that positive or negative charges changed the interfacial orientation of ions — the ions in the first layer tended to orient parallel to the surface, while counterions in the second shell became preferentially oriented perpendicular to the surface. The structural changes in the interfacial region consequently affected the electrostatic interactions.[106]

Intermolecular forces can be directly measured by atomic force microscopy (AFM). For example, AFM force-distance measurements carried out on a system of gold nanoparticles in imidazolium ionic liquids showed a stepwise repulsive force when two gold-coated surfaces approached each other within a few nanometers.[84] This stepwise force-distance curve indicated an ionic layer present around the nanoparticle surface that provided electrostatic force.[84]

The Derjaguin-Landau-Verwey-Overbeek (DLVO) theory[110], which has been frequently applied to quantitatively calculate the stability of colloidal dispersions, considers a combination of electrostatic double layer repulsion (Coulomb forces) and van der Waals attraction to examine the colloidal stability. The total particle-particle interaction energy potential (V_{total}) is calculated by addition of the van der Waals potential (V_{vdW}) and the electrostatic potential (V_{ele}):

$$V_{total} = V_{vdW} + V_{ele} \quad (1)$$

In an example of DLVO theory utilization, the potential between two gold NPs (with a diameter of 6 nm) dispersed in 1-butyl-3-methylimidazolium bis(trifluoromethylsulfonyl)imide ([Bmim][Tf_2N]) was calculated by adding the electrostatic potential and the van der Waals potential. A negative total potential over the whole distance range resulted, indicating an unstable colloidal system. [84]

An approximate expression (when κR>>1) for the electrostatic

repulsion potential $V_{ele}(d)$ is:[111]

$$V_{ele} = 2\pi R\,\varepsilon_0\varepsilon_r\psi_0 \ln\left[1+\exp(-\kappa d)\right] \quad (2)$$

where Ψ_0 is the surface potential.

The Debye reciprocal length parameter, κ, can be calculated from:[112]

$$\kappa = \left(\frac{\sum_i (z_i e)^2 c_{i0}^*}{\varepsilon_0\varepsilon_r kT}\right)^{1/2} \quad (3)$$

where z_i stands for ion valence, e is elementary charge, c_{i0}^* is the bulk concentration of ions (at a reference point where the potential equals zero), ε_r is the solvent dielectric constant, and ε_0 is the permittivity of free space. k is the Boltzmann constant and T is the absolute temperature.

Given all the other constants, a static permittivity (ε) of 11 was used to calculate $V_{ele}(d)$ and κ, and a zeta potential of -55 mV was used as a good approximation of the surface potential (Ψ_0) in ionic liquids.[84] The thickness of the Debye layer (1/κ) can be utilized as a measure of colloidal electrostatic stability.[112] The colloidal particles are more stable with a thicker Debye layer because it expands the distance between nanoparticles, reducing the chance for nanoparticle agglomeration. Moreover, a wider separation between nanoparticles reduces van der Waals interactions, which further discourages nanoparticle aggregation.[59]

The $V_{vdW}(d)$ potential between two spherical particles of radius R can be approximated by:[84]

$$V_{vdW} = -\frac{R}{12d}\left[\left(\sqrt{A_m}-\sqrt{A_p}\right)^2\right] \quad (4)$$

A_p is the Hamaker constant of particle, A_m is the Hamaker constant of the colloidal medium. A_p and A_m can be calculated based on Lifshitz theory:[113]

$$A = \frac{3}{4}kT\frac{(\varepsilon-1)^2}{(\varepsilon+1)^2} + \frac{3h\nu_e(n^2-1)^2}{16\sqrt{2}(n^2+1)^{3/2}} \quad (5)$$

where ε is the dielectric constant and n is the refractive index of the compound, and ν_e is the frequency of the main electronic absorption for the dielectric permittivity. Values for these properties for a variety of commonly used ionic liquids and nanoparticles are available in literature.[88] The dielectic constant can be measured by, e.g., microwave dielectric relaxation spectroscopy[114], while refractive indices can be measured using a refractometer with a high-resolution optical sensor[115]. The value for ν_e is typically around 3×10^{15} s^{-1} for ionic liquids.[116]

From equations 2 to 5 we can see that the electrostatic and van der Waals interactions are computed as a function of the distance (d) between neighboring particles. The distance (d) can be calculated via the nanoparticle size and concentration, parameters related to physicochemical properties of each ionic liquid (ε, n, ν_e), and environment temperature (T).

First, the distance between neighboring particles (d) is a key independent variable contributing to the magnitude of electrostatic and van der Waals interactions. The interaction potential profiles for gold NPs and silica nanoparticles in ionic liquids calculated through DLVO showed that the magnitude of both electrostatic and van der Waals interactions decreases sharply with d increase.[84, 88] It was observed that larger silica nanoparticles were unstable in a series of aprotic ionic liquids, while smaller silica nanoparticles (with radius of 6 nm) were stable in 1-butyl-3-methylimidazolium tetrafluoroborate ([Bmim][BF_4]), indicating an increase in the van der Waals attraction with increasing nanoparticle size.[51]

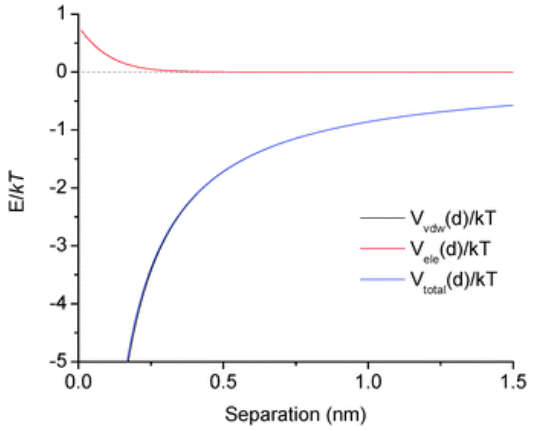

Figure 9. The total interaction potential $V_{total}(d) = V_{vdw}(d) + V_{ele}(d)$ as a function of distance between two spherical gold particles with a diameter of 6 nm in [Bmim][Tf_2N]. A dashed line at zero potential is drawn for clarity. The electrostatic interactions decrease to negligible amount within the distance of 0.25 nm and are weaker than 1 kT over the whole distance range, while the van der Waals interactions start from a distance of more than 10 nm and become stronger than 1 kT at 1 nm interparticle distance.[84] Copyright 2012 the Owner Societies.

Second, the physicochemical properties of ionic liquids and nanoparticles, reflected in the parameters used in equations 2-5, e.g., dielectric constant and refractive index of ionic liquids, differ from each ionic liquid and result in changes in the value for electrostatic and van der Waals interactions. For example, assuming the dielectric constant of ionic liquid A to be larger than that of ionic liquid B, the Debye reciprocal length parameter, κ, for A will be smaller than that for B according to the relationship $\kappa \propto (1/\varepsilon_r)^{1/2}$. The electrostatic potential of a nanoparticle in ionic liquid A will be higher than that in ionic liquid B with a larger Debye screening length, consequently this nanoparticle should be more stable in ionic liquid A all else being equal.

Finally, other than the distance between neighboring nanoparticles and the physicochemical properties of ionic liquids, temperature is an important parameter in calculating electrostatic and van der Waals interactions since the Hamaker constants (of both ionic liquid and nanoparticle) and the Debye reciprocal length are a function of temperature (Eq. 3 and Eq. 5). A temperature increase would lead to a Debye reciprocal length decrease, and, as a result, electrostatic interactions would increase. From this aspect, the thickness of the electrical double layer would increase with a decrease in Debye reciprocal length, which would separate the neighboring nanoparticles further, and, as a consequence, the van der Waals interactions would weaken. Moreover, temperature also indirectly impacts van der Waals and electrostatic interactions through affecting the physicochemical

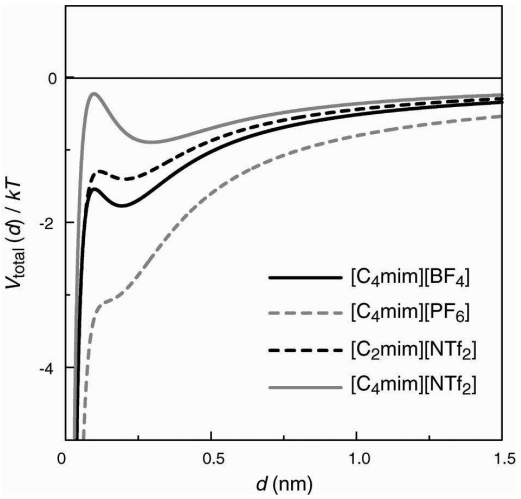

Figure 10. DLVO interparticle interaction profiles (T =25 °C) for bare silica particles (R = 60 nm) in [$C_n$mim])-based ionic liquids. All the potential curves were negative over the entire range of interparticle distance, indicating that the total interactions are attractive over the entire range and the nanoparticles are not stable.[88] Copyright 2008 American Chemical Society.

properties of ionic liquids and nanoparticles.

Figure 9 shows the total potential as well as the van der Waals and the electrostatic potentials (expressed in units of kT) as a function of distance between two spherical gold particles immersed in [Bmim][Tf_2N]. The Hamaker constant A_m for [Bmim][Tf_2N] = 5.57×10^{-20} J and the Hamaker constant A_p for gold = 1.26×10^{-19} J. The result indicates that the electrostatic interaction decreases to negligible amount within a distance of 0.25 nm and is smaller than 1 kT over the whole distance range, while the van der Waals interaction commences from a distance of more than 10 nm and becomes greater than 1 kT at 1 nm interparticle distance. The theoretically calculated interaction potential vs. separation distance curve is in good agreement with AFM results.[84] Figure 10 shows the total interaction profiles of silica nanoparticles in 1-alkyl-3-methylimidazolium ([$C_n$mim]$^+$)-based ionic liquids calculated through the DLVO theory.[88] All the potential curves were below the zero potential over the entire range of interparticle distance covered in the figure. In other words, the silica nanoparticles attracted each other, suggesting that the silica nanoparticles were electrostatically unstable in the ionic liquids used. A broader size distribution and larger particle radius were measured by DLS at 12 h after sample preparation, as expected by the DLVO prediction. The results suggest the possibility that the electrostatic repulsion is attenuated by the highly ionic atmosphere in ionic liquid media.[88]

The DLVO theory has been widely applied to colloidal dispersions in molecular solvents.[112, 117] DLVO interactions in ionic liquid-based colloidal systems are different than those in molecular solvents with minimal to zero ionic strength. Equation 4 indicates that the van der Waals potential is dominated by the effective Hamaker constant, defined as $A_{eff} = (A_m^{1/2} - A_p^{1/2})^2$. The effective Hamaker constants of ionic liquid-silica nanoparticle colloidal systems (A_{eff} ([$C_n$mim])-based ionic liquids-silica) = ~ 3-7× 10^{-22} J) were reported smaller than those of aqueous or typical organic colloidal dispersions of silica particles (A_{eff} (water-silica) = 36.2×10^{-22} J and A_{eff} (acetonitrile-silica) = 29.5×10^{-22} J), which indicated that the attractive van der Waals interactions for silica nanoparticle and ionic liquid systems were weaker than those of aqueous or typical organic solvent colloidal dispersions.[88] Equation 3 suggests that the electrostatic interaction is related to the bulk concentration of ions, c_{i0}^* The estimated high values of c_{i0}^* of ionic liquids (>1.5 mol L^{-1}), resulting from the partially associated ions, lead to a substantially suppressed Debye length κ^{-1} in ionic liquids, and subsequently caused electrostatic interactions to decline.[51] Compared to ionic liquid-based colloidal systems, the electrostatic repulsion is stronger in dilute electrolyte aqueous solution, which presents a higher energy barrier for nanoparticles to aggregate. The electrostatic repulsion declined dramatically when the surface charges decreased or when the concentration of the electrolyte solutions increased in aqueous solution, resulting in a lower energy barrier that triggered slow particle aggregation.[118]

Despite its wide use and many successes, the classic DLVO theory has several limitations emanating from its assumptions, e.g., dilute solution, no multiple charges, and no hydrogen bonding.[110] DLVO only considers additive electrostatic forces and van der Waals interactions. In more complicated systems, interactions other than electrostatic and van der Waals exist and significantly effect colloidal stability. In this case, non-DLVO forces, or extended DLVO (EDLVO)[119] forces have to be taken into consideration.[120] Adjustments should be made to the DLVO theory and necessary complements should be added considering the hydrogen bonds and steric interactions in ionic liquids. For example, the potential interactions within a suspension of oleate-coated iron-based magnetic particles (with average diameter of 9.04 ± 0.08 nm) in [Emim][$EtSO_4$] ionic liquid were theoretically predicted by extending the DLVO theory with considerations for steric repulsion and magnetostatic attraction between two particles.[100] Similar to electrostatic interactions, the structural interactions are provided by the solvation layers surrounding the nanoparticles, yet they are different in terms of origin. The structural interactions will be reviewed in the next section, and other non-DLVO interactions will be discussed in the sections that follow.

2.3 Structural interactions

In colloidal systems the motion of the solvent molecules surrounding the particle surface is constrained within a narrow range. Solvation shells are built by proton-donors and proton-acceptors forming hydrogen bonds, and by electrostatic interactions attracting counterions. For aqueous colloidal systems, this orientation restriction is indicated as hydration pressure and the solvation shell is referred as hydration shell.[120] In dispersions of nanoparticles in ionic liquids, ion shells are built around nanoparticles to effect stabilization through structural forces. The nanoparticles can be viewed as encapsulated in constraining nanoregions of ionic liquids.[121] The solvation layers are squeezed out of the closing gap when two solid surfaces approach each other, thus providing structural repulsion to prevent nanoparticles from agglomerating. The constraining effect on solvent molecules/ions and the attractive interactions between nanoparticle surface and solvent molecules/ions hence generate solvation forces between neighboring nanoparticles.[122] The structural forces between nanoparticles and ionic liquids can be

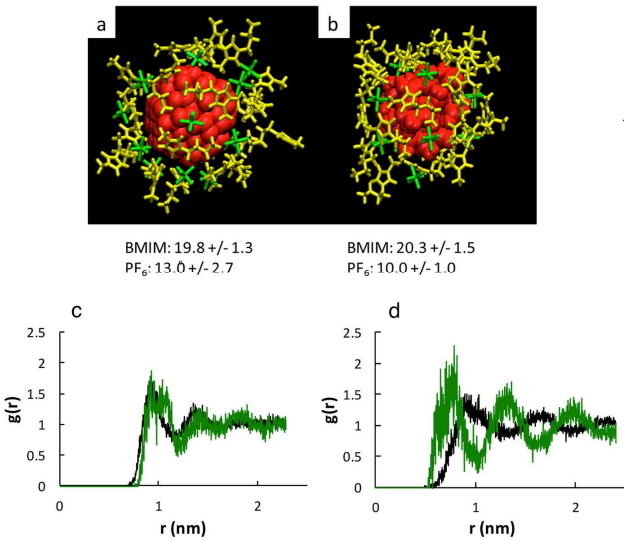

Figure 11. IL solvation shells around a (a) hydrocarbon and (b) silica nanoparticle. [Bmim][PF_6] are represented by stick structure, and nanoparticles are represented as dark red circles. The radial distribution functions of the $[Bmim]^+$ cation (black) and the $[PF_6]^-$ anion (green) with respect to the centers of mass of (c) the hydrocarbon and (d) the silica nanoparticles.[123] Copyright 2003 The Royal Society of Chemistry.

assessed by evaluating these solvation layers. X-ray spectroscopy and scattering, including X-ray absorption spectroscopy (XAS), X-ray photoelectron spectroscopy (XPS), and small-angle X-ray scattering (SAXS), are often used to probe the formation of the solvation layers.[52]

Take negatively charged silica nanoparticles in an ionic liquid as an example. At first, the cations of the ionic liquid are attracted to the nanoparticle surface by attractive electrostatic forces, while also by hydrogen bonding with the silanol group. Outside of the first layer, the ionic liquid anions are attracted by the positive cations to form a second layer, wherein hydrogen bonds also form between ionic liquid cations and anions. A similar mechanism forms the third and forth and more layers, resulting in an ionic liquid-based supramolecularly structured shell that surrounds the nanoparticles.[124, 125] AFM results from the EAN-silica system showed at least five solvation layers to be present.[124] The number of layers is highly affected by surface charge, surface roughness, and orientation of the cations in the interfacial layer. Among different materials (mica, silica, and graphite), the material (silica) with the lower surface charge and higher roughness led to less strongly bound solvation layers, which decreased the number of detectable solvent layers.[124] A recent study on the colloidal stability in EAN of maghemite nanoparticles (γ–Fe_2O_3, median radius of 3.4 nm) with various counterions on their surfaces indicated that the presence of counterions at the nanoparticle surface altered the colloidal stability compared with electrically neutral maghemite nanoparticles. The results indicated that the various counterions modified the repulsive interaction potential between the colloids, especially the structural interactions, through forming the very first cationic layer around the nanoparticles and subsequently affecting the ionic liquid solvent layers. However the modification of interfacial microstructure is only indirectly evidenced in this case, and a straightforward explanation of ion-dependent colloidal stability has not been achieved due to limited previous studies on salt effects in nanoparticle/ionic liquid colloidal systems.[126, 127]

Molecular dynamics simulations provide a more direct way to "observe" the solvation shell at a molecular level. Figure 11 shows the result of a MD simulation of the ionic liquid ([Bmim][PF_6]) solvation layer around a hydrocarbon nanoparticle (consisting of carbon atoms with 1.2 nm in diameter and saturated with CH, CH_2, and CH_3 groups) and a silica nanoparticle (with 1.1 nm diameter and surface saturated with silanol groups). The radial distribution functions (rdf) of the $[Bmim]^+$ cation and the $[PF_6]^-$ anion with respect to the centers of mass of the hydrocarbon and the silica nanoparticles are shown in Figure 11(c) and (d). The oscillatory rdfs of the cation and anion surrounding the hydrocarbon nanoparticle overlapped each other, suggesting that both ions contribute to the solvation layers with similar behavior, with $[Bmim]^+$ cations slightly closer to the hydrocarbon nanoparticle surface. In contrast, the oscillations of the cation and anion rdf around the silica nanoparticle were highly mismatched, indicating that the solvation layers consisted of alternating ions. The results suggested that all the ions played a role in the solvation shell mainly due to electrostatic attraction, despite the different hydrophobicites of the hydrocarbon and the silica nanoparticles and ions.[123]

2.4 Solvophobic interactions

The hydrophobic force is another non-DLVO force acting in aqueous colloidal systems that is considered as a factor of affecting colloidal stability.[120] In the case of ionic liquid-based colloidal systems, we refer to this as solvophobic force. Analogous to polymers in a bad solvent, the nanoparticles tend to aggregate so as to reduce the contact area with the ionic liquid in the case where the nanoparticle surface is solvophobic relative to the ionic liquid medium. In order to explore the effects of solvophobic interactions on nanoparticle stability, the dispersion stability of silica nanoparticles (primary particle domain size between 10 and 20 nm, with silanol groups on the surface) was considered in hydrophilic ([C_6mim][BF_4]) and hydrophobic ([C_6mim][NTf_2]) ionic liquids.[128] A better dispersibility indicated by Newtonian fluid-like rheological behavior in the hydrophilic ionic liquid at room temperature and at 100 °C, even at higher nanoparticle concentrations, implied that the hydrophilic silica nanoparticles with silanol groups were more stable at the solvophilic conditions. To further confirm this, the silica nanoparticles were surface functionalized to render them hydrophobic. The hydrophobic silica nanoparticles in the hydrophobic ionic liquid behaved like Newtonian fluids, indicating better dispersibility.[128] A similar study has been conducted on dispersions of titania nanoparticles in a hydrophilic ([Emim][BF_4]) and a hydrophobic ([Emim][Tf_2N]) ionic liquid. The Newtonian fluid-like behavior and smaller aggregation size suggested that hydrophilic TiO_2 nanoparticles, owing to their surface hydroxyl groups, were better dispersed in [Emim][BF_4].[129] A very recent study conducted by the same group considered another oxide with broad applications, ZnO (with particle size of 14.9±0.2 nm or 46.6±2.0 nm). DLS and rheological characterization indicated that the nanoparticles dispersed better in the hydrophilic ionic liquids [Emim][BF_4],

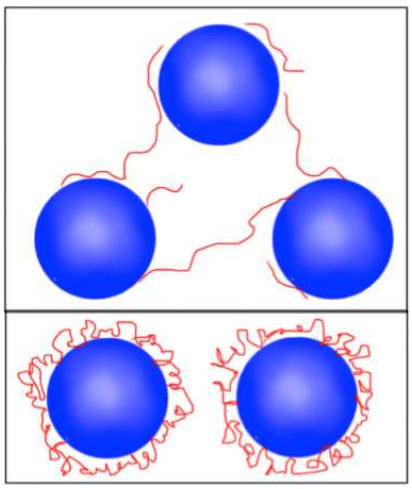

Figure 12. Polymers provide steric forces between nanoparticles. The top panel shows polymers functioning as bridges between nanoparticles when small amounts of polymer are added to the nanoparticle-ionic liquid dispersion. The bottom panel shows polymers fully covering the nanoparticle surface to form a polymer layer when an excess of polymer is added to this system.

[Bmim][BF_4], and 1-hexyl-3-methylimidazolium tetrafloroborate [C_6mim][BF_4].[130]

Besides the direct influence of solvophobic forces, the relative solvophibicites of ionic liquids and nanoparticles having surface-grafted polymers can impact the colloidal stability through steric interactions, which will be discussed next (Section 2.5).[88, 100]

2.5 Steric interactions

When two nanoparticles having polymers adsorbed on their surface approach each other, the polymer layers may undergo some compression resulting in a strong repulsion that is referred to as steric interaction.[122] The physical basis of steric repulsion is a combination of entropic and osmotic contributions. The entropic contribution is due to a volume restriction effect that decreases possible configurations in the region between two surfaces. The osmotic effect arises from a difference in concentration of the adsorbed polymers in the region between the two surfaces as they approach closer.[120] Steric interactions in colloidal dispersions in molecular solvents have been extensively studied.[122, 131-134] In ionic liquid-based colloidal systems, steric forces can emerge from bulky groups within a molecule and/or from addition of macromolecules, both of which hinder nanoparticles from physically contacting each other and/or from forming chemical bonds.

When small amounts of polymer are added to the nanoparticle-ionic liquid dispersion, the nanoparticle surfaces are partially covered by polymers, where polymer coils extend from one particle surface to another particle and make molecular contact. In this way polymers can function as bridges between nanoparticles. As an excess of polymer is added to this system, the polymers can fully cover the nanoparticle surface to form an adsorbed polymer layer[135] (Figure 12). Steric repulsions arising from the adsorbed polymer layers of neighboring nanoparticles "push" nanoparticles away from each other. Block copolymers have been utilized to stabilize nanoparticle dispersion.[131] Taking aqueous media as a comparison, a monolayer of poly(ethylene oxide)-poly(propylene oxide)-poly(ethylene oxide) (PEO-PPO-PEO) block polymer (Pluronic F127) was reported to surround carbon black particles (100-120 nm in diameter and with surface oxidized in small portion to form COO- groups) below the critical micelle concentration (CMC), while micelle-like block copolymer assemblies adsorbed on the carbon black particles above the CMC.[136]

Compared to structural forces, which originate from the solvation layer being squeezed out of the closing gap when two solid nanoparticles approach each other, steric forces originate from polymers or side chains attached at the solid–liquid interface dangling out into the solution where they remain thermally mobile.[122] In the cases of nanoparticles in pure ionic liquid without polymer addition, the ionic liquid provides structural forces through forming solvation layers. However, if the ionic liquid comprises long alkyl side chain, e.g., from imidazolium- or pyrazolium- based cations, the cations being attracted near nanoparticle surfaces can provide steric forces by stretching out their bulky side-chains, thus hindering the nanoparticles from approaching each other. This effect is steric rather than structural. A study on the stabilization of bare silica nanoparticles in imidazolium-based ionic liquids found that adjusting the affinity between the ions and particle surfaces by carefully selecting the ions of ILs and/or the nanoparticle surface modification could optimize the ionic liquid-based steric stabilization provided by the nonpolar alkyl chains as a protective group.[51] We have discussed in Ch. 2.2 about the stable dispersion of negatively charged gold nanoparticles in ionic liquids based on cation-only electrostatic stabilization.[108] In addition to the electrostatic stabilization, steric interactions also contribute to nanoparticle stabilization due to the arrangement of the long side-chain attached to the imidazolium ring. Surface-enhanced Raman spectroscopy (SERS) spectra suggested that the ionic liquid cation rings oriented parallel to the gold nanoparticle surface, while the long side-chains stretched far away from the nanoparticle surface, impeding the nanoparticles from approaching each other. The van der Waals forces between nanoparticles strongly diminished as a result of the increase of mean distance between gold nanoparticles, which further prevented the nanoparticles from agglomeration.[108]

The difference in polarity and the hydrogen-bonded supramolecular structure with cation and anion aggregates engender microheterogeneity in ionic liquids.[43, 137] The semiorganized ionic liquid-based nanostructure that extends beyond the electrostatic double layer also leads to steric forces that stabilize the embedded nanoparticles. A schematic of metal nanoparticles stabilized in an ionic liquid network structure is presented in Figure 13.[59, 125] The $[(Bmim)_{x-n}(PF_6)_x]^{n-}$ and $[(Bmim)_x(PF_6)_{x-n}]^{n+}$ supramolecular ion aggregates provide steric hindrance in addition of electrostatic forces stabilizing the gold nanoparticle. (Figure 8)[109]

Besides the steric forces afforded by ionic liquids with long side-chains, stronger steric interaction could be achieved by the addition to the ionic liquid medium of polymers or surfactants. Magnetite nanoparticles (with mean diameter of 7.4 ± 1.3 nm, coated with oleate) dispersed in the ionic liquid [Emim][$EtSO_4$] with addition of oleic acid proved to be more stable compared to similar hybrids without surfactant (oleic acid) addition.[100] The

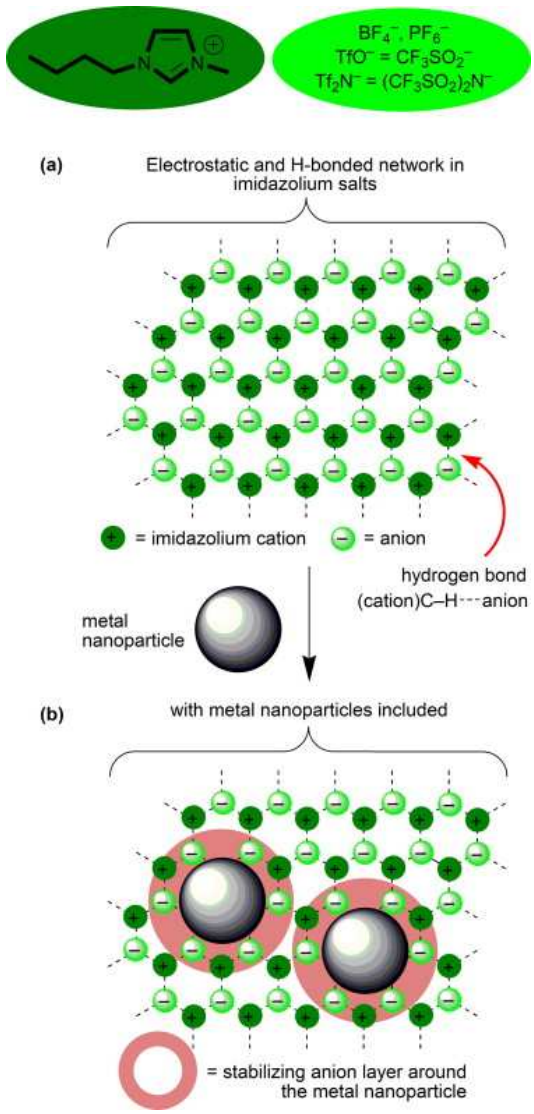

Figure 13. (a) Schematic of network structure in 1,3-dialkylimidazolium-based ionic liquids. (b) Inclusion of metal nanoparticles (M-NPs) in the supramolecular IL network with electrostatic and steric stabilization is indicated through the formation of a suggested primary anion layer around the M-NPs.[59] Copyright 2011 Elsevier.

oleic acid tends to form a double layer via hydrophobic interactions when sufficient amount of oleic acid is added to the magnetite nanoparticle ionic liquid suspension. The oleic acid stretches out on the surface of magnetite nanoparticles, offering steric repulsion to achieve effective stabilization.[100] The steric repulsion was calculated from the equations,[100]

$$V_s(r)=\begin{cases} 2\pi kTR^2\xi\left[2-\dfrac{l+2}{t}\ln\left(\dfrac{1+t}{1+l/2}\right)-\dfrac{l}{t}\right], & \\ \qquad\qquad r/2s\le 1 & \\ 0, \qquad\qquad r/2s>1 & \end{cases} \tag{6}$$

with $l=\dfrac{r}{R}$; $t=\dfrac{s}{R}$.

where R is the radius of the particle, s is the thickness of the adsorbed layer, and ξ is the surface concentration of the adsorbed molecules, which is calculated by considering the packing density of the adsorbed surfactants.

Polymers have long been used as stabilizers in colloidal systems based on the steric interactions that they provide.[120] The steric repulsion provided by polymers is highly determined by the affinity of polymer to the dispersion medium, which is ionic liquid in our case. Gold nanoparticles (diameter not specified) dispersed in neat [Bmim][PF_6] (the total gold concentration was 1.1 mM) are steric stabilized to some degree by the butyl- side chain on the imidazolium ring, appearing to be very stable for a week, while minimal aggregation was observed later.[83] However, UV-vis and TEM results showed these gold nanoparticles to be much more stable (for periods of several months) upon addition of poly(vinylpyrrolidone) (PVP，MW＝40,000).[83] A subsequent study also confirmed that, while short-term stability of gold nanoparticles can be achieved in imidazolium-based ionic liquids with predominant electrostatic stabilization, the addition of an extra stabilization agent, e.g., PVP, greatly enhanced the nanoparticle colloidal stability.[138]

Apart from physical adsorption on the nanoparticle surface to provide steric forces, ionic liquids and polymers can be chemically bonded to the nanoparticle surface, making possible steric repulsion by stretching out bulky molecular groups into the solvent. Nanoparticle surfaces are regularly modified to achieve certain properties by the choice of grafted polymers.[139] In good solvent conditions, the grafted polymers tend to expand and stretch out to the ionic liquid media, providing steric repulsion to keep nanoparticles from approaching each other.[88] On the other hand, at bad solvent conditions, the grafted polymers contract on the nanoparticle surface,[120] allowing a decrease in the distance between neighboring nanoparticles and an increase in the van der Waals forces, which, in return, renders the nanoparticle dispersion unstable. The stability of poly(methylmethacrylate) (PMMA)-grafted silica nanoparticles (PMMA-g-NPs) in ionic liquids with different anions has been examined.[88] The PMMA-g-NPs phase-separated in [Bmim][BF_4], which is a bad solvent for PMMA. On the other hand, TEM results confirmed that PMMA-g–NPs were stably dispersed with a narrow size distribution in [$C_n$mim][NTf_2] and [Bmim][PF_6], which are good solvents for PMMA.[51, 88] The hydrodynamic radius of PMMA-g-NPs was found a good measure of the solubility of PMMA in 1-alkyl-3-methylimidazolium ionic liquids.[140]

The steric interaction potential (V_{steric}) was calculated based on an intimate mixing of the grafted polymers arising from two different particles in the ILs:[88]

$$V_{steric}\propto\left(\frac{1}{2}-\chi\right) \tag{7}$$

where χ is the Flory-Huggins interaction parameter[112], which accounts for the mixing free energy (ΔG_{mix}) of the ionic liquid solutions of PMMA, and can be written as:

$$\chi=\frac{v_m}{RT}(\delta_{polymer}-\delta_{IL})^2 \tag{8}$$

where v_m is the molar volume of solvent (ionic liquid) and δ is the Hildebrand solubility parameter.

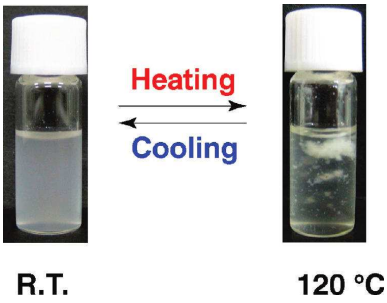

Figure 14. Photographs of 1 wt % PBnMA-grafted silica nanoparticle colloidal suspension in [Emim][NTf_2] at room temperature (R.T.) (left) and at 120°C (right). At room temperature, the nanoparticles remain stably dispersed in ionic liquid. At 120°C, PBnMA-grafted silica nanoparticles completely phase-separated from ionic liquids. Because of the lower density of nanoparticles than [Emim][NTf_2], the aggregates can be seen in the upper part of the sample.[141] Copyright 2010 American Chemical Society.

The Flory-Huggins interaction parameter is smaller than 0.5 in a good solvent but larger than 0.5 in a poor solvent.[112] According to Eq. 7, the steric interaction is repulsive (positive potential) in a good solvent and is attractive (negative potential) in a poor solvent. Values of the Flory-Huggins interaction parameter for PMMA in [Bmim][BF_4] and [Bmim][PF_6] are calculated by eq. 8 as 11.7 and 10.1, respectively,[142] while χ is 6.62 in [Bmim][NTf_2],[143] indicating that all these ionic liquids are bad solvents for PMMA. Unfortunately, the calculated values of the Flory-Huggins interaction parameter contradict the experimental results of PMMA-g-NPs in ionic liquids. To explain this, it was argued that ionic liquids are assumed to be a one-component solvent in previous calculations of the Flory-Huggins interaction parameter, while ionic liquids are dissociated into cations and anions in an actual situation.[88] It is important to develop a judicious way to predict the Flory-Huggins interaction parameter for steric interaction calculations of polymer-grafted nanoparticles in ionic liquids.

Temperature affects the steric forces between nanoparticles by influencing the solubility of grafted polymers in ionic liquids. At room temperature, a colloidal suspension of poly(benzyl methacrylate) (PBnMA)-grafted silica nanoparticles was found very stable with the grafted PBnMA chains stretching out into [Emim][NTf_2] ionic liquids providing strong steric stabilization. However, at a higher temperature (120 °C), the grafted PBnMA cannot dissolve in this ionic liquid, thus could not provide sufficient steric forces to stabilize the colloidal suspension, consequently leading to aggregation as shown in Figure 14.[141]

Steric stabilization of nanoparticles provided by polymer grafting is also utilized to modify the ionic liquid and nanoparticle hybrids in order to increase tolerance for other solvents, e.g., water. Bare iron oxide nanoparticles (with diameter at around 8.2~10.6 nm) were found stable in both protic ethylammonium and aprotic imidazolium room-temperature ionic liquids for several months, however they became very unstable with even small amount of water (e.g., in the case when residual water remained in the ionic liquid following vacuum pumping).[144] Following the formation of an effective steric barrier by grafted short poly(acrylic acid)-b-poly(acrylamide) copolymer that is compatible with the ionic liquid, the iron oxide

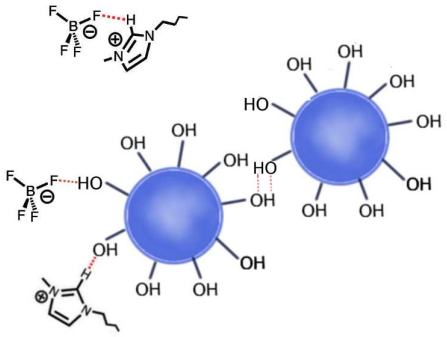

Figure 15. Hydrogen bonds formed between the surface hydroxyl- groups of nanoparticles and ions of ionic liquids, and between cations and anions of ionic liquids.

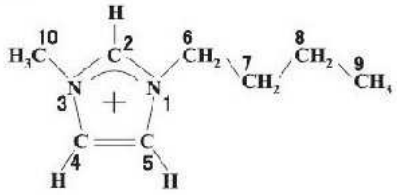

Figure 16. Chemical structure of 1-butyl-3-methylimidazolium cation. Carbon atoms are numbered as indicated in the figure.

nanoparticles and ionic liquid mixtures could achieve high stability over the whole range (0-100 %w/w) of water concentration.[145] Such a high water tolerance provides an inspiration to explore further ways to stabilize nanoparticles in ionic liquids in the presence of water and/or other impurities, which are frequently encountered in practical applications.

2.6 Hydrogen bonding interactions

Hydrogen bond interactions are necessary to be considered in ionic liquid-based colloidal systems in addition to the classic electrostatic and van der Waals interactions. Several ionic liquids are highly hydrogen bonded to form supramolecular structures.[7, 37, 41] In such ionic liquids, the cations contain one or more proton donors, which could form X-H…Y hydrogen bonds with halogen containing anions, e.g., $[BF_4]^-$, $[PF_6]^-$. Some nanoparticles possess hydroxy- and/or oxy- moieties on their surface, e.g., silica nanoparticles have silanol groups (—Si—OH), which can also hydrogen bond with ionic liquids.[146] The cation-anion hydrogen bond and NP-IL hydrogen bond compete with each other and contribute to nanoparticle stabilization in ionic liquids, as shown in Figure 15.[87, 105, 129] Hydrogen bonding density has been reported as a useful indicator of solvation.[147]

As a hydrogen bond forms between atom-attracting sites with different electronegativity, the hydrogen atom covalently bonded with a more electronegative atom interacts with the atom bearing lone electron pairs.[148] The electronegativity of the atom covalently bonded with hydrogen is called hydrogen bond acidity.[120] The hydrogen-bond donation abilities (HBDA) of ionic liquids can qualitatively convey their acidities. On the contrary, the specific electronegativity of heteroatoms bearing lone electron pairs is captured by the hydrogen bond basicity.[149] The hydrogen bond basicity can be measured by solvatochromic characterization.[150] Both hydrogen bond acidity and basicity are

Table 1. Values of hydrogen bond acidity (α) and hydrogen bond basicity (β) of commonly used ionic liquids and molecular solvents.

compound	α	β
[Bmim]Cl	0.41	0.95
[Bmim]Br	0.36	0.66
[Bmim][CH_3SO_4]	0.59	0.65
[Bmim][BF_4]	0.63	0.38
[Bmim][PF_6]	0.63	0.21
[Bmim][Tf_2N]	0.62	0.24
[Pyr][Tf_2N]	0.48	--
[$(C_4H_9)(CH_3)_3N$][Tf_2N]	0.47	--
water	1.53	1.237
methanol	0.92	1.423
1-butanol	0.89	1.49
dimethyl sulfide	0.24	1.048

α and β values of [Bmim]-based ionic liquids are from reference[151], α values of [Pyr][Tf_2N] and [$(C_4H_9)(CH_3)_3N$][Tf_2N] are from reference[41], α and β values of water, methanol, 1-butanol and dimethyl sulfide are from reference[149].

good indicators of hydrogen bond strength.[150]

With the same anion, the HBDA values of pyridinium-based ionic liquids (0.48 for [Pyr][Tf_2N]) and quaternary amino ionic liquids (0.47 for [$(C_4H_9)(CH_3)_3N$][Tf_2N] are smaller than those of imidazolium-based ionic liquids (0.66 for 1,3-dialkylimidazolium bis(trifluoromethylsulfonyl)imide), suggesting that the hydrogen bond interactions of pyridinium-based and quaternary amino-based ionic liquids are not as remarkable as those of imidazolium-based ionic liquids.[41] For the commonly used 1-alkyl-3-methylimidazolium-type ionic liquids, hydrogen bonds can be formed with the C2, C4 and C5 carbons on the imidazolium thing, especially on the most acidic C2 position[152] (see Figure 16). Table 1 lists values of hydrogen bond acidity (α) and hydrogen bond basicity (β) of some commonly used ionic liquids and molecular solvents, from where we can see that the molecular solvents have higher basicity in general, while the acidity varies over a wide range.

The hydrogen bonds that form between nanoparticle surfaces and ionic liquid cations and anions are likely to compete with each other in nanoparticle/ionic liquid hybrid systems. Theoretically, the greater the acidity and basicity of the hydrogen bonding atoms, the stronger the hydrogen bond would be. The strength and length of hydrogen bonds, like other chemical bonds with fundamental vibrational frequencies that are on the order of kT, are sensitive to the environment temperature and pressure.[153] Since the hydrogen bond is directional, the steric configuration, such as a bulky side chain, may obstruct hydrogen bond formation.[154]

The occurrence and intensity of hydrogen bonds in colloidal systems are usually characterized by infrared (IR) spectra.[67, 146] The hydrogen bond formation within silica nanoparticles dispersed in imidazolium-based ionic liquid system was studied under ambient and high pressure.[146] A comparison of the IR spectra of 1-ethyl-3-methylimidazolium bis(trifluoromethylsulfonyl)amide ([Emim][TFSA]) / nanosilica mixture with that for pure [Emim][TFSA] showed that the formation of certain C-H…silica hydrogen bonds or C-H…O hydrogen bonds between the alkyl C-H/imidazolium C-H of ionic liquid and the surface of silica nanoparticles provided stabilization for the nanoparticle dispersion.[146] The remarkable red shifts and band splitting of the IR spectra observed for the mixture with 10 wt% silica nanoparticles at pressure > 1 GPa indicated that the high pressure-enhanced hydrogen bond between ionic liquid and silica nanoparticle competed with cation-anion hydrogen bonds, resulting in ionic liquid microstructure phase transition from associated clustering to dissociated, thus stabilizing the nanoparticles inside the ionic liquid.[146] Similar results were also reported for TiO_2 nanoparticles dispersed in 1-ethyl-3-methylimidazolium trifluoromethanesulfonate ([Emim][TFS]) ionic liquid: high pressure contributed to the stabilization of the TiO_2 nanoparticles by the formation of pressure-enhanced imidazolium C-H…TiO_2 hydrogen bonds, which perturbed the ionic liquid local structure.[67]

2.7 Effect of water on interactions in ionic liquid media

Water impurities have been a big issue in the history of ionic liquid research and applications.[21, 26, 155-157] Among ionic liquids commonly used nowadays, those with tetrafluoroborate, hexafluorophosphate, and nitrate anions, and imidazolium-based cations have noticeable interaction with water through hydrogen bonding, thereby are prone to absorb moisture from air, something that destabilizes dispersed nanoparticles.[158-161] Because water has comparatively low molecular weight, it can be present in chemically significant molar concentrations even inside hydrophobic ionic liquids.[159, 162, 163] The water concentration affects the nanoparticles stability in ionic liquids in two aspects: (i) water addition alters the DLVO, steric, and solvophobic interactions between nanoparticles and ionic liquids through affecting the ionic liquid nanostructure and physicochemical properties;[156, 164-166] and (ii) water molecules penetrate the ionic liquid solvation layers to directly interact with the nanoparticles[144].

For trace amounts (ppm) of water present in ionic liquids, interactions between water and the anions of the ionic liquids lead to changes in the structure of water.[167] Experiments showed that $[BF_4]^-$ provided stronger interactions with water than $[PF_6]^-$ by forming hydrogen bonds or by inducing hydrogen bonds among water molecules.[161] In the case of trace amount of water addition in ionic liquid and nanoparticle hybrid systems, such small amount of water cannot influence the bulk properties, instead water molecules penetrate the ionic liquid solvation layer to directly interact with the nanoparticles.[84, 107] The presence of water (actual amount not reported) destroyed the ionic liquid double layer surrounding the nanoparticle and the ionic liquid supramolecular structure.[107] Gold nanoparticles (diameter ranging from small primary clusters (<2.5 nm) to larger NPs (4–7 nm), at concentration of 320 mmol Au per mol IL after 1 min sputtering) aggregated and sedimented in [Bmim][Tf_2N] with water content as low as 2 ppm. These gold nanoparticles in [Bmim][Tf_2N] with 100 ppm water sedimented faster and coagulated more than in the

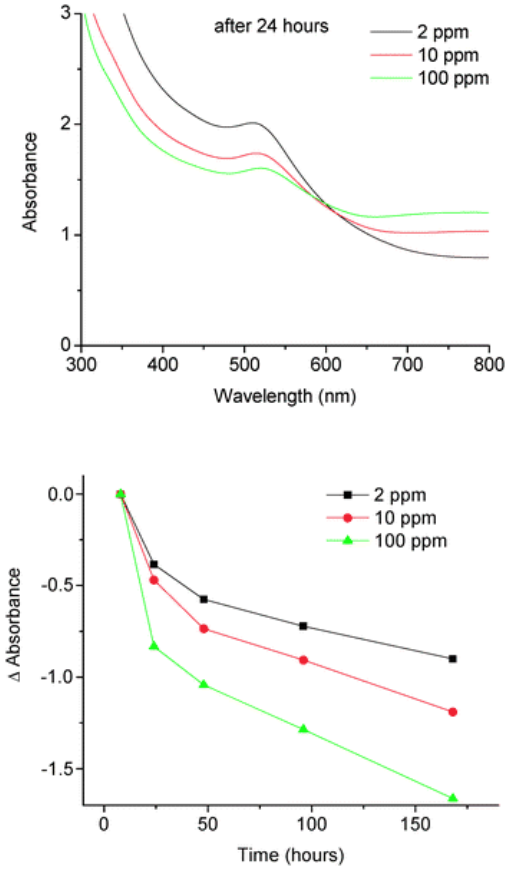

Figure 17. (top) UV-vis absorption spectra of gold nanoparticles (diameter ranging from small primary clusters (<2.5 nm) to larger NPs (4–7 nm)) dispersed in mixtures of the ionic liquid [Bmim][Tf_2N] with different water contents after 24 hours. (bottom) Change in absorbance at 520 nm for different water contents as a function of time after gold nanoparticles were synthesized by physical vapor deposition (sputtering) in ionic liquid.[84] Copyright 2012 the Owner Societies.

system with 10 ppm water, which, in turn, sedimented faster and coagulated more than in the system with 2 ppm water, as shown in Figure 17. In this case, at a water content of 10 ppm, water molecules were estimated to cover 70% of the gold nanoparticle surface.[84] The hydrophilic property of gold nanoparticles attracted the water molecules from the bulk to the vicinity of the nanoparticles, which caused a relatively high water concentration near the nanoparticle surface and affected the stabilizing force of the ionic liquid surrounding the nanoparticle.[84] A study on the stability of silica nanoparticles (500 nm radius) in water and EAN mixtures showed that the addition of even small amounts of water (at the lowest investigated water concentration of 5 wt %) reduces both the number and resilience of EAN solvation layers around silica particles.[168] Weak solvation forces were detected by AFM in the mixtures with 90 and 95 wt % EAN, however these weak solvation forces were not sufficiently strong to prevent nanoparticle aggregation on long time scales.[168] In another study, the stability of spherical polystyrene latex particles (surface-modified by amidine with a radius of 110 nm, or surface-modified by sulphate with a radius of 265 nm) was examined in several imidazolium- and pyrrolidinium-based ionic liquids.[169] The results of time-resolved light scattering indicated that the aggregation rate decreased rapidly with increasing IL content at

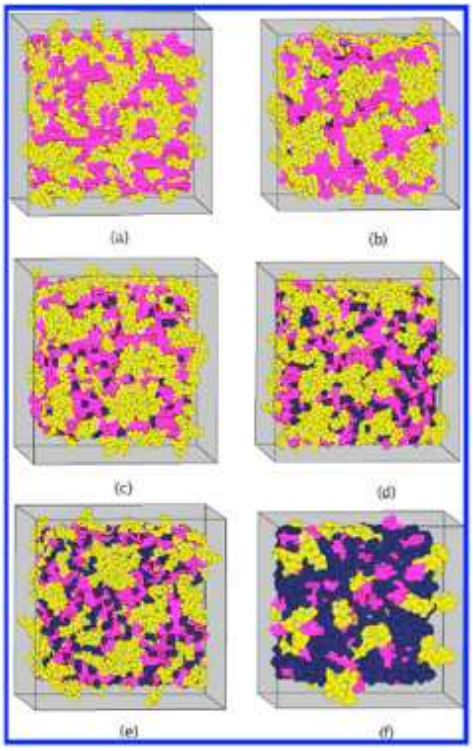

Figure 18. Snapshots of six selected simulation cells, taken from MD trajectory data. The polar groups, nonpolar groups, and water are colored red (grey), yellow (light), and dark, respectively. (a) Dry 1-octyl-3-methylimidazolium nitrate ionic liquid sample, Mixture with water of (b) 20%, (c) 50%, (d) 75%, (e) 80%, (f) 95.2% mole fraction.[170] Copyright 2007 American Chemical Society.

high (around 1) IL-to-water molar ratios, suggesting a slow aggregation resulting from progressive screening of the solvation layers.[169] A study on magnetic fluids stated that water molecules could screen the protective layer formed by $[(Bmim)_2(BF_4)_3]^-$ supramolecular aggregates surrounding the maghemite nanoparticles.[144] Additionally, the ionic liquid semiorganized layer was destroyed due to the water affinity of the BF_4, resulting in maghemite nanoparticle aggregation and the instability of the colloidal dispersion. This study further suggested that the water affinity of ionic liquids (especially anions) and the size of anions significantly affected the stabilization of nanoparticle and ionic liquid hybrid systems.[144] Another study confirmed that Ag nanoparticle dispersion in [Bmim][BF_4] were prone to aggregation and precipitation (to form aggregates with length of around 400 nm) even in the presence of small quantities (actual amount not reported) of water.[107]

At higher amounts (more than trace) of water present in ionic liquids, water can affect the nanoparticle colloidal stability in two aspects---change in ionic liquid nanostructure and physicochemical properties. The physicochemical properties of ionic liquids, such as dialectic constant, density, viscosity, refractive index, and polarizability, are dependent on the amount of absorbed water,[171] which further affect the stability of dispersed nanoparticles in several ways through acting on the intermolecular forces as we have discussed in sections 2.2-2.6 (eq.2-5 and eq.7-8). A clustering of the ionic liquid in alkyl regions occurs in mixtures of [Bmim][BF_4] with water.[172]

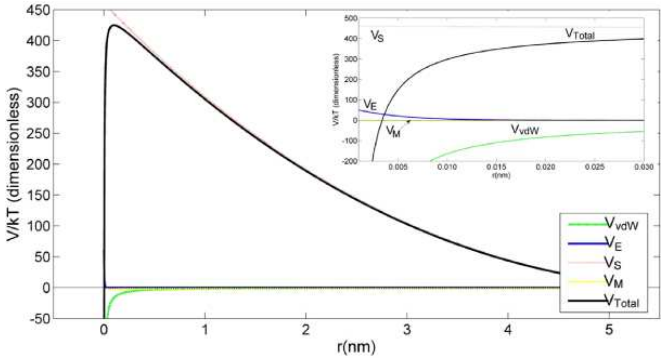

Figure 19. Interaction potentials for magnetite nanoparticles (with mean diameter of 7.4 ± 1.3 nm) chemisorbed with oleate in [Emim][$EtSO_4$] with oleic acid addition, calculated by an extension of the DLVO theory, where V_{vdW} is the potential of van der Waals interactions, V_E is the potential of electrostatic interactions, V_S is the potential of steric interactions, V_M is the potential of magnetic forces, and V_{Total} is the total interaction potential.[100] Copyright 2011 IOP Publishing Ltd.

[Bmim][BF_4] was reported to aggregate like a surfactant at low concentrations (with CMC at around 0.8 M) in water.[173-175] X-ray scattering investigation on the effect of water on a series of protic ionic liquids showed that the ionic liquid aggregates were stable in size upon dilution (with IL molar fraction between 0 and 0.3), indicating that the water is localized in the ionic region and has little effect on the nonpolar domains, while at high ionic liquid concentrations (with IL molar fraction between 0.3 and 1), there was a significant proportion of perturbed water, indicating that water is influenced in some way by the IL cations and anions.[176] Figure 18 shows results of molecular dynamics simulations of water concentration effects on the nanostructure of water and 1-alkyl-3-methylimidazolium ionic liquid mixtures.[170] The effect of water on the stabilization of silica particle (500 nm radius) suspensions was assessed using dynamic light scattering and optical microscopy in pure water, various water-EAN mixture and pure EAN.[168] The silica particles dispersed in pure EAN and pure water were well stabilized by electrostatic forces provided in pure water and by solvation forces (chapter 2.3) provided in pure EAN, whereas the silica particles formed large aggregates in all water-EAN mixtures considered. AFM results showed a purely attractive force profile in the water-EAN mixtures containing 5 to 75 wt % EAN, which indicated that there was no barrier to particle-particle contact and this resulted in rapid particle aggregation.[168]

2.8 Interaction balance and competition

We have reviewed in previous sections separately each of the major interactions affecting the stability of nanoparticle dispersions in ionic liquids. However, instead of each interaction acting on nanoparticles independently, these interactions work in tandem to cause stable/unstable colloidal systems.

To compare how various interactions act on the stability of nanoparticle and ionic liquid colloidal systems, we give here an example on a stable dispersion of 9.5 vol % magnetite nanoparticles (7.4 ± 1.3 nm mean diameter, with chemisorbed oleate) in [Emim][$EtSO_4$] with 23 wt% oleic acid added.[100] The total interaction potential, consisting of van der Waals, electrostatic, steric repulsion, and magnetostatic energy potentials, was calculated by adding the different contributions, as $V_{Total}(r) = V_{VdW}(r) + V_E(r) + V_M(r) + V_S(r)$. The van der Waals potential, electrostatic potential and steric repulsion potential were calculated as a function of the distance between the particle surfaces, r, using the equations discussed in sections 2.2-2.5. The potential profiles are shown in Figure 19. This figure clearly shows that the electrostatic interaction is too weak compared to van der Waals attraction, in which case the nanoparticles can be expected to aggregate in the absence of additional interactions. The result of eq. 6 showed the steric potential to decrease as the distance increases between neighboring nanoparticles. The steric potential was much higher than other interactions especially in close distances. In this case, the steric repulsion provided by oleic acid addition was high enough to overcome all the attractive forces, contributing majorly to stabilize the nanoparticle in ionic liquids by raising the total interaction potential to an effective potential barrier (higher than 400 kT) against aggregation.[100]

The overall interaction profile of nanoparticle dispersion in ionic liquids obtained by molecular dynamics (MD) simulations (with necessary assumptions and parameters) provides a way to theoretically assess the colloidal stability.[105, 177] Molecular simulations quantified the interaction energy between ruthenium nanoparticles (RuNPs, with mean diameter of 1.1 ± 0.2 nm and 2.3 ± 0.6 nm) and [Bmim][Tf_2N] and other imidazolium-based ionic liquids, and revealed the distribution of the ions and of electrostatic charges surrounding the nanoparticle.[105] The results suggested that RuNPs interacted favorably with ionic liquids having longer alkyl side chains, which enhanced the van der Waals interactions with RuNPs. Compared to [Bmim][Tf_2N], ionic liquids with an additional methyl group on the C2 carbon of the cation have lower propensity to form H-bonds, which attenuated the interactions with RuNPs. The overall interaction profile was a balance between electrostatic, van der Waals, and hydrogen bond forces.[105]

Endogenous and exogenous variables, including nanoparticle size and concentration, physicochemical properties of ionic liquids, temperature and pressure, act on different intermolecular interactions at the same time. For example, van der Waals, electrostatic and steric interactions are all functions of the distance between neighboring nanoparticle surfaces. Taken all interactions into consideration, the total interaction curve displays a positive maximum peak at a distance on the order of the nanoparticle diameter.[88, 100] The rheology of silica nanoparticle (with primary diameter of 10-20 nm, hydrophobicaly surface modified with trimethoxypropylsilane (TMPS) or chlorotrimethyl-silane (CTMS)) dispersions in imidazolium-based ionic liquids changed with the concentration of the nanoparticles. The dilute (up to 1 wt%) silica nanoparticle dispersions behaved like Newtonian fluids in hydrophobic ionic liquids, where the viscosity is independent of the shear rate. Dispersions of the same nanoparticles at higher concentrations were found unstable, and the viscosity depended on the shear rate, suggesting the presence of agglomerates.[128, 129]

Physicochemical properties of ionic liquids impact the stability of nanoparticle dispersion in ionic liquids. According to Eq. 2-5, the Hamaker constants of nanoparticles and ionic liquids play important roles in van der Waals interaction. Electrostatic interactions and structural interactions originate from cations and

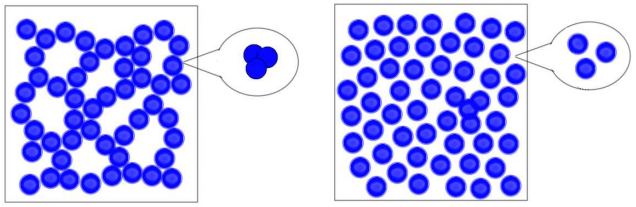

Figure 20. Schematics of colloidal gel and colloidal glass. In colloidal gels (left), the dispersed nanoparticles touch each other to form an interconnect network structure. In colloidal glasses (right), the concentrated dispersed nanoparticles get very close to each other without collision in a way that the nanoparticles are trapped within cages by neighboring nanoparticles.

anions forming solvation layers, thus the physicochemical parameters that affect the solvation layer (Debye length), e.g., solvent dielectric constant, would be important to the electrostatic and structural interactions. The solubility parameters of ionic liquids and the added/grafted polymer can capture the steric interactions between nanoparticles. It has been suggested[95] that the differences in gold nanoparticle formation and stabilization in the different ionic liquids examined (based on 1-ethyl-3-methyl-imidazolium cation and different anions) was a result of a combination of ionic liquid physicochemical parameters, among which the density, viscosity and dielectric constant were main factors to consider. A lower dielectric constant could be advantageous for the stabilization of the gold nanoparticle dispersion, while other physicochemical parameters of the ionic liquids might play less important roles or were unable to be directly evidenced in this study.[95]

Temperature affects the nanoparticle dispersion in ionic liquids through van der Waals, electrostatic, steric and hydrogen bond interactions, which we have discussed in detail in sections 2.2, 2.5, and 2.6, respectively. With quantitative support from UV-vis data, a study on gold nanoparticle formation in $[Emim]^+$-based ionic liquids found that at increasing temperature (180 °C), more and more gold particles aggregated into relatively well-ordered supracrystalline aggregates.[95]

3. Nanoparticle organization in ionic liquids

In the previous chapter, we discussed intermolecular interactions acting within dispersions of nanoparticle in ionic liquids. In general, relatively low concentrations of nanoparticles can stably disperse in suitable ionic liquids stabilized by a balance of several intermolecular interactions, or by the addition of polymers that provide extra steric force. On the other hand, unstable or concentrated nanoparticle dispersions can form homogeneously distributed soft materials under certain circumstances.[51] Instead of being randomly dispersed into a liquid, nanoparticles can be incorporated into a solid-like structure of lyotropic liquid crystals (LLC) formed by the ionic liquids and/or added amphiphiles. In what follows we first introduce the formation of colloidal glasses and colloidal gels, and the transition between them. Then we discuss the selective localization of nanoparticles synthesized/dispersed in different ionic liquid-based LLC structures. Last, we review other cases of nanoparticle organization with ionic liquids, including nanoparticle-stabilized ionic liquid containing emulsions, ionic liquid surface-functionalized nanoparticles, and nanoscale ionic materials.

3.1 Colloidal gels and glasses in ionic liquids

Several types of solid-like soft materials based on nanoparticles dispersed in ionic liquids have been obtained recently, more notably colloidal gels and colloidal glasses. A colloidal gel is attained by the dispersed phase forming an interconnect network structure,[178] while a colloidal glass is formed when high concentration dispersed nanoparticles are trapped from moving by neighboring nanoparticles through a "cage effect".[51] (Figure 20)

Colloidal gels formed by a three-dimensional nanoparticle and/or polymer network percolated throughout the ionic liquid are denoted as ionogels, which hybridize the properties of ionic liquid with those of another organic, inorganic or hybrid organic–inorganic component.[179] [180] In this review we focus on the ionogels that are built through nanoparticle networks. Ionogels can be prepared by suspending unstable nanoparticles into ionic liquids, within which the repulsive forces between nanoparticles are weaker than the attractive forces. The required nanoparticle concentration for colloidal gelation depends on the size of the nanoparticles. In the case of larger silica nanoparticles (300 nm diameter), 40 wt% silica particles were required for gelation in $[Emim][Tf_2N]$, whereas 5 wt% silica nanoparticles with 12 nm diameter were required to achieve gelation.[51] In this colloidal system, the very high ionic strength of ionic liquids penetrates the screening shell of the nanoparticle surface charges, resulting in inefficient interparticle electrostatic repulsion. Consequently the silica nanoparticles aggregate in ionic liquids.[88] Diamond nanoparticles (average diameter <10 nm) formed a gel from 10 wt% with a variety of ionic liquids, including $[Bmim][PF_6]$, $[Bmim][Tf_2N]$, 1-butyl-3-methylimidazolium hexafluoroantimonate ($[Bmim][SbF_6]$) and $[Bmim][BF_4]$.[181]

For nanoparticles that are surface-modified with grafted polymers, the affinity between the grafted polymers and the ionic liquid solvents impacts the stability of the nanoparticle dispersion. The steric forces between neighboring nanoparticles diminish when the grafted polymers contract to reduce the solvophobic interactions between polymer and the ionic liquid that acts as a bad solvent.[88] The unstable polymer-grafted nanoparticles attach to each other and form ionogels over time.[141] Systems comprising PMMA-grafted silica nanoparticles in $[Emim][Tf_2N]$ transformed from liquid to solid with color change in the range from 0 to 33.3 wt% nanoparticles.[51] Similarly to polymer-grafted nanoparticle gelation in ionic liquids, ionic liquid-grafted nanoparticles could also form gels in another ionic liquid. A novel class of silica nanoparticle-based ionogels was created by dispersing silica nanoparticles densely grafted with the ionic liquid 1-trimethoxysilyl propyl-3-methyl-imidazolium bis-(trifluoromethylsulfonyl) imide ([Spmim][TSFI]) in the 1-butyl-3-methyl-pyrrolidinium bis(trifluoromethylsulfonyl) imide ([Bmpyr][TFSI]) ionic liquid host. The [Spmim][TSFI]-grafted silica nanoparticles remained stable in [Bmpyr][TFSI] over the wide concentration range of 0-70 wt% nanoparticle. The resulting ionogel exhibited liquid-like ionic transport properties over an extended temperature range (with a crystallization temperature below -60 °C, depending on the nanoparticle concentration).[182]

Colloidal glasses form when the repulsive forces are very

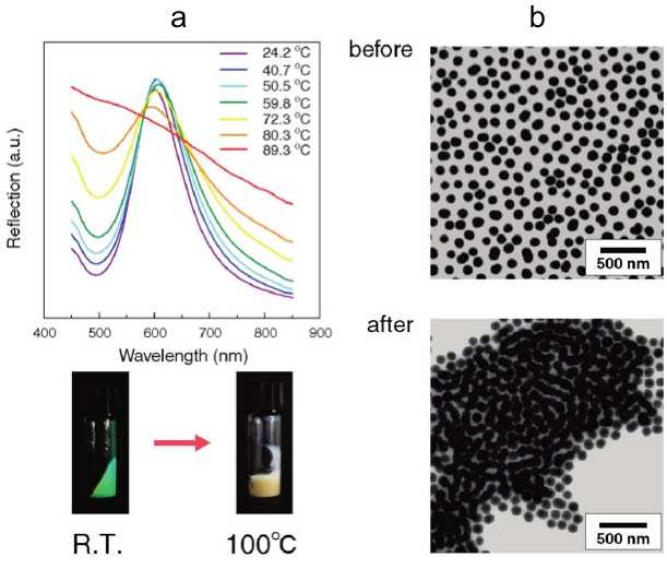

Figure 21. (a) Reflection spectra of 25 wt % PBnMA-based silica nanoparticle (with core diameter of 120 nm) with [Emim][NTf_2] ionic liquid colloidal glass at different temperatures. Structural color changes before and after heating from room temperature (R.T.) to 100 °C. (b) TEM images of 25 wt% PBnMA-based colloidal glass before (top) and after (bottom) heating to 100 °C. Reproduced from ref[141]. Copyright 2010 American Chemical Society.

strong even in concentrated nanoparticle dispersions in ionic liquid. At high volume fractions, nanoparticles occupy limited volumes of solvent in a concentrated system, but cannot attach to each other due to the strong repulsive forces. They get very close to each other without collision in a way that the nanoparticles are trapped within cages formed by the neighboring nanoparticles, like the way that atoms array in metals. The cage effects are also the reason for the solid-like properties of colloidal glass.[51] Compared to colloidal gels/ionogels, colloidal glasses form when the grafted polymers have a good affinity for the ionic liquid they are dispersed in, in which case the polymers stretch out from the nanoparticle surface into the ionic liquid providing steric repulsion. Sterically stabilized PMMA-grafted silica nanoparticles (with silica core radius of 61 nm) in [Emim][NTf_2] ionic liquid (good solvent) exhibited liquid-like behavior at dilute suspensions, but solidified as the suspension become more concentrated (above 14 wt% nanoparticles) and exhibited different colors depending on the particle concentration as a consequence of the structural color.[51]

Colloidal glasses and colloidal gels formed by polymer-grafted nanoparticles in ionic liquids would experience reversible phase transition between glass phase and gel phase if the solubility of the polymer in the ionic liquid was sensitive to environment change, e.g., temperature. A thermosensitive nanoparticle grafted with poly(benzyl methacrylate) (PBnMA) was designed on the base of the PMMA-grafted silica nanoparticles mentioned above.[51] PBnMA is soluble in the [Emim][NTf_2] ionic liquid at lower temperatures but insoluble at temperatures higher than the phase-separation temperature (Tc). When PBnMA-grafted silica nanoparticles were used instead of PMMA-grafted silica nanoparticles, the nanoparticle suspension in [Emim][NTf_2] became unstable at high temperature (above 90 °C) due to contraction of the grafted polymer. In dilute solution, the nanoparticles formed aggregates as the high temperature decreases the dispersion stability. For a concentrated suspension of colloidal glass at low temperature, the steric force diminished rapidly as the grafted polymers contracted, and as a result the nanoparticles were able to attach to each other and form a network. A V-shaped rheological response of the temperature dependence of storage modulus and loss modulus for PBnMA-based colloidal glass in [Emim][NTf_2], which results from a reduction in the particle volume fraction of the colloidal glass, suggested that the short-range-ordered colloidal glass structure was transformed into a completely disordered structure at higher temperatures. A change in the optical properties upon heating, along with the rheological response, confirmed the colloidal glass to gel transition.[51] Further study indicated that the interparticle interaction changed from repulsive to attractive at the lower critical solution temperature (LCST) of PBnMA, thus causing a temperature-induced colloidal glass-to-gel transition (Figure 21).[141]

Acting as structuring media for inorganic ionogel formation, the intrinsic organization and physicochemical properties of ionic liquids influence the network building,[179] resulting in ionic liquid-based colloidal gels with many potential applications, especially in batteries, due to good ionic conductivity while maintaining solid-like rheological response.[179, 180] A high ionic conductivity of approximately 10^{-2} S cm^{-1} at 30 °C despite of the solid-like behavior, which is comparable to that of neat [Emim][NTf_2], was obtained at a low silica concentration (5 wt%) ionogels.[183] Meanwhile, viscoelastic responses, such as shear-thinning and shear-induced sol-gel transitions, were observed in all of the silica nanoparticle-based ionogels containing 5-15 wt% silica nanoparticles.[183] A stimulus-responsive glass-to-gel transition is a noteworthy property that may contribute to various applications, such as thermo-sensitive detectors.

3.2 Nanoparticle localization in ionic liquid-based long-range structures

Ionic liquids with long side alkyl chains exhibit amphiphile-like features due to the combination of a nonpolar alkyl chain part and a polar cation head group (usually heterocyclic group). As a result, long alkyl chain ionic liquids are able to form long-range ordered liquid crystalline (LC) structures at the molten state, while they form lyotropic liquid crystalline (LLC) phases in the presence of solvents including other ionic liquids.[175, 184, 185] Spherical $Mn_{1,5}[Cr(CN)_6]$ nanoparticles (with a mean diameter of ~4.0 (±0.6) nm, with 0.03 mol/L $Mn_{1,5}[Cr(CN)_6]$ in the system) were synthesized in ionic liquid crystals formed by an imidazolium-based ionic liquid with properly chosen N-alkyl substituent and counteranion, 1-dodecyl-3-methylimidazolium tetrafluoroborate, [C_{12}mim][BF_4]. This nanoparticle and ionic liquid-based lamellar liquid crystal composite was an opaque yellow solid at room temperature. X-ray, polarized optical microscopy (POM) and TEM results suggested that the nanoparticles were organized into parallel chains in hydrophilic layers along with water, $[BF_4]^-$ and imidazolium ring entities, while the alkyl side chains of the ionic liquids formed hydrophobic layers.[186] On the other hand, a system comprising the same nanoparticles synthesized in a similar way in

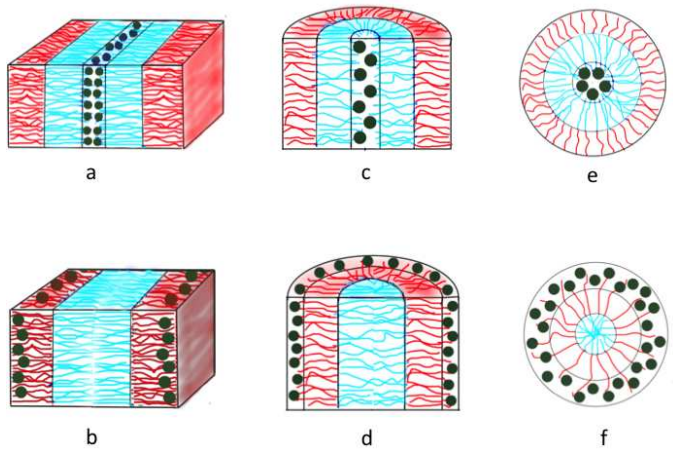

Figure 22. Schematic representation of nanoparticles selectively located in ordered structures formed by amphiphiles. (a) and (b) lamellar structure; (c) and (d) cylindrical structure; (e) and (f) spherical structure. Red/blue (dark/light) lines represent hydrophobic/hydrophilic part of amphiphile, dark dots represent nanoparticles.

$[C_{10}mim][BF_4]$ remained a yellow viscous liquid without liquid crystal formation at room temperature, with the nanoparticles randomly dispersed in the isotropic ionic liquid.[186] Another relevant study investigated multi-walled carbon nanotubes dispersed in LLC structures formed by binary mixture of 1-tetradecyl-3-methylimidazolium chloride (C_{14}mimCl) and EAN ionic liquids. A multi-walled carbon nanotube (with diameter of 10–20 nm and length of 10–15 μm, at a concentration of 0.014%) dispersed in the hexagonal, cylindrical (H_1) phase without disrupting the ionic liquid structure. However, larger lattice spacing upon nanoparticle incorporation was measured by SAXS, indicating a dispersion of carbon nanotubes (CNT) into the cylinder-like assemblies of the H_1 structure. Such CNT-LC composite is expected to exhibit remarkably high electrical conductivity resulting from great conductivities of both the carbon nanotube and the ionic liquid crystal.[187]

In addition to the formation of LC or LLC structures by neat or mixed ionic liquids, lyotropic liquid crystals formed by the self-assembly of concentrated amphiphiles (including surfactants, lipids or block copolymers) in ionic liquids[58, 188] can be utilized as matrices for nanoparticle synthesis.[188, 189] EAN dispersion of 0.2 wt% multi-walled carbon nanotube was added to a preformed hexagonal LLC phase of 50 wt% nonionic polyoxyethylene surfactant $C_{16}EO_6$ in EAN. Polarized optical microscopy images combined with SAXS indicated that the multi-walled carbon nanotubes were well dispersed in the hexagonal LLC without destroying its structure. This LLC composite of uniform dispersion of multi-walled carbon nanotubes was still stable after six months without any precipitation or phase separation. A uniform distribution of spherical Ag nanoparticles was obtained from inherent reduction of $AgNO_3$ in a lamellar liquid crystal formulated by the ionic liquid [Bmim][PF_6], Tween 85 (Polyoxyethylene Sorbitan Trioleate) and water. The nanoparticle diameter was in the range 3-10 nm depending on the thickness of the solvent layer of the lamellar phase (<10 nm in this case).[190] PEO-PPO-PEO block copolymer Pluronic P123 ($EO_{20}PO_{70}EO_{20}$) formed lamellar lyotropic liquid crystal structure in pyrrolidinium nitrate ([Pyrr][NO_3]) ionic liquid at the 58-82 wt% polymer concentration range. Gold nanoparticles were prepared by reducing $HAuC_{l4}$ in this lyotropic liquid crystal, leading to an increase by 0.7 nm in the repeat distance for the lamellar phase presumably due to the swelling effect of gold nanoparticles formed in this LLC phase.[90]

The formation of nanoparticle-LLC composites was based on the interplay between the particle-particle excluded-volume interactions, preferential particle/block interactions, and the enthalpic and stretching interactions within the block.[191, 192] The morphology of such self-assembled ordered mesophases depends on the characteristics of both amphiphiles and nanoparticles.[193] Figure 22 presents some possible locations of nanoparticles incorporated in ordered structures formed by amphiphiles.

The lyotropic liquid crystal structures formed by a given amphiphile in aqueous solution and in ionic liquids are slightly different under the same condition. For example, 60 wt% Pluronic P105 PEO-PPO-PEO block copolymer formed hexagonal structure in both water and EAN, however the lattice parameter obtained in water was higher than that in EAN. In addition, the lattice spacing of the P105-EAN LLC structure did not change with an amphiphile concentration increase, which was different from the observations in water.[194, 195] These differences emanate from the solvent preferred interactions with the PEO block over the PPO block, which is affected by the hydrophobicity and the hydrogen bond interaction between PEO with EAN and these between PEO and water.[188] However, to our best knowledge, no comparisons have been made between systems where nanoparticles are dispersed in lyotropic liquid crystal structures formed by the same amphiphile in water and in ionic liquids.

3.3 Other soft materials based on nanoparticle and ionic liquid hybrids

Various forms of organization have been developed comprising ionic liquid and nanoparticle ingredients. As discussed previously, by simply dispersing nanoparticles into ionic liquids, one may achieve stable nanoparticle dispersions, colloidal gels or colloidal glasses, depending on the intermolecular interactions, and, further, nanoparticles can be dispersed into preformed structures such as LLCs assembled by ionic liquids or amphiphiles. Other than dispersion, other types of nanoparticle and ionic liquid hybrid materials can be attained through nanoparticle-stabilized ionic liquid-containing emulsions or nanoparticle surface functionalization with ionic liquids.

Nanoparticles can be localized at ionic liquid-based interfaces in ionic liquid-water/oil emulsions.[196] An ionic liquid ([Bmim][BF_4])-in-castor oil microemulsion containing as-prepared copper nanoparticles, which were formed on the interface of microemulsion droplets and then transported into the ionic liquid phase, was reported to exhibit high stability after storage for 6 months at ambient conditions.[197] The inner and outer droplets of these emulsions, including oil-in-ionic liquid, ionic liquid-in-oil, and three-component multiple emulsion, could be controlled by altering the volume fractions of the liquid components and the concentrations of the stabilizing particles.[198] To investigate ionic liquid microemulsions that involve solid nanoparticles as emulsion stabilizers, hydrophobic nanoparticles (spherically modified hydrocarbon nanoparticles with mean diameter of 1.2 nm) at ionic liquid-water and ionic liquid-oil

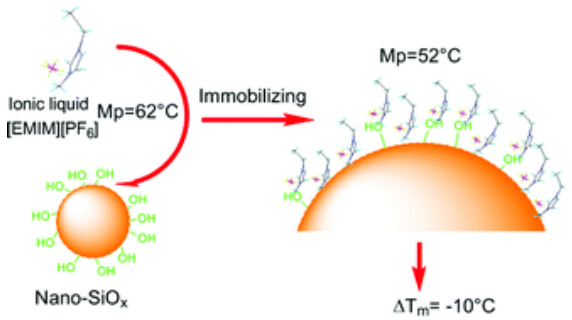

Figure 23. Schematic of ionic liquid [EMIM][PF_6] immobilized on a silica surface. The ionic liquid-immobilized SiOx nanoparticles have lower melting points compared to the bulk ionic liquids, as indicated in the schematic.[199] Copyright 2010 The Royal Society of Chemistry.

interfaces were studied using molecular dynamics simulations.[177] The nanoparticles were initially dispersed in the water phase, and then rapidly approached the [Bmim][PF_6] ionic liquid-water interface, consequently the majority of the nanoparticles entered into the ionic liquid phase. The width and morphology of the ionic liquid-water interface changed significantly to accommodate the presence of nanoparticles. For the [Bmim][PF_6]-hexane system, the nanoparticles were initially dispersed in the hexane phase and primarily remained there. The ionic liquid-hexane interface remained undisturbed although the nanoparticles slowly approached the interface. This result may be explained by the competition between [Bmim] cations and water/hexane for the nanoparticle surface based on different hydrophobicity.[177] A similar study was conducted on silanol-saturated hydrophilic nanoparticles in the same ionic liquid-water and ionic liquid-oil systems. It turned out that the silica nanoparticles maintained equal volume in both phases as for ionic liquid-water system, while they completely partitioned into the ionic liquid phase in the case of the ionic liquid-oil system.[123] The results have met the expectations of strong association between nanoparticles and solvents of similar hydrophobic nature.[123] Novel emulsions containing ionic liquids have been extensively studied over the recent years.[196] We have reviewed above some representative examples that focused on nanoparticle-stabilized emulsions. The emulsions with high surface areas enable fast mass transfer and can provide significant advantages in applications utilizing ionic liquids as solvents in two-phase systems.[198] Besides forming hybrid materials based on nanoparticle-stabilized ionic liquid- water/oil emulsions, ionic liquid-based emulsions are also useful as nanoparticle synthesis media.[200-202]

Nanoparticles can be surface modified/functionalized by ionic liquids through physical adsorption or covalent grafting to the nanoparticle surface to improve desired properties, e.g., better dispersibility, better thermo-stability. Novel functional materials with hybridization of ionic liquids and nanoparticles have been prepared in order to share the properties of both ionic liquids and nanoscale materials. For example, ionic liquids/silica nanocomposites produced by a phosphonium-type ionic liquid reacting with silica nanoparticles have good dispersibility in a variety of solvents and great thermal stability even at 800 °C.[203] Carbon nanotubes chemically modified by imidazolium-based ionic liquids with Cl^- or Br^- counterions are dispersible in water, while those modified with imidazolium-based ionic liquids with $[BF_4]^-$, $[PF_6]^-$ counterions are able to disperse in organic solvents such as $CHCl_3$.[204] Chemical bonding of nanoparticles with ionic liquids also modifies the physicochemical properties of ionic liquids. Imidazolium-based ionic liquids immobilized onto the surface of SiO_x nanoparticles (Figure 23) were reported to have lower melting points compared to the bulk ionic liquids, which is mainly due to the interfacial interaction between nanoparticles and the formation of intermolecular hydrogen bonds between the anions of ionic liquids and the silanol groups on the surface of SiO_x nanoparticles. The interfacial interactions (van der Waals) between the immobilized ionic liquid and SiO_x nanoparticle decreased the mobility of ionic liquid cations near the nanoparticle surface so as to trap the cations at a higher entropic state, which lead to the melting temperature decrease.[199] A high degree of conformational ordering of the ionic liquids on the surface of SiO_x nanoparticles was attained as a result of limited degrees of freedom of the dialkyl imidazolium cation due to chemical bonding between the ionic liquid and the nanoparticle surface.[199]

Within the general field of grafted nanoparticles, nanoscale ionic materials (NIMs) comprise a nano-sized particle core and an oppositely charged canopy through ionic coupling. The core of NIMs is surface functionalized with a charged corona, which can be one portion of an ionic liquid.[205] The dynamic nature of the ionic links brings up one of the primary characteristics of NIMs - the similarity of their structural and dynamic behavior to that of ionic liquids.[206] NIMs are also referred as nanoscale ionic liquids, as they share properties with ionic liquids, including an ionic attraction between the components in NIM, a low-to-nonexistent vapor pressure, and a high density of ionic groups.[205, 206] NIMs prepared by surface modification of silica cores by an alkylsilane monolayer paired with an amine-terminated poly(ethylene oxide)-poly(propylene oxide) block copolymer canopy exhibited liquid-like behavior under ambient conditions in the absence of solvent, which is believed due to the rapid exchange of the block copolymer canopy with the ionically modified silica cores.[207] Liquid-like NIMs can act as functional ionic liquids and as surface functionalized nanoparticle dispersions, and offer potential applications in various fields, such as lithium-ion batteries, carbon-capture materials and catalysts.

4. Concluding remarks

Ionic liquid and nanoparticle hybrids have attracted attention recently due to their unique characteristics and broad potential applications. Studies on the intermolecular interactions affecting the stability of ionic liquid-based nanoparticle dispersions and on the "interaction force – structure – function" relationships in nanoparticle-ionic liquid composites provide fundamental knowledge needed for the rational design of such materials and their applications under various working environment. In this review, we discuss the stability of nanoparticle dispersion in ionic liquids and the organization of nanoparticle in ionic liquids as affected by intermolecular interactions, along with other forms of ionic liquid and nanoparticle hybrids and their applications.

The stability of ionic liquid and nanoparticle hybrid systems provides information on the rational design of materials and proper selection of operating conditions. The characterization

methods used to assess the stability of ionic liquid-based colloidal systems are similar with those of general colloidal systems. However, the intermolecular interactions between nanoparticles and ionic liquids, which dictate the nanoparticle stability, differentiate such hybrids from those within aqueous or organic solvent-based colloidal systems. In ionic liquid media, electrostatic repulsions tend to be attenuated by a highly ionic atmosphere, and the hydrogen bond basicity in general is lower than that of molecular solvents, however, hydrogen bonds can form on several positions of an ionic liquid cation or anion. Further, ionic liquids with long side-chains provide steric stabilization in addition to solvation forces. Endogenous variables and exogenous variables, e.g., physicochemical properties of ionic liquids and nanoparticles, temperature and pressure, and water concentration, affect the stability of nanoparticle dispersion in ionic liquids through each interaction. Among the various interactions, van der Waals, electrostatic and steric interactions are well established and can be quantified as functions of neighboring nanoparticle distance, whereas hydrogen bonding and structural forces are less studied quantitatively and are mostly evaluated in a qualitative manner.[113] Therefore, a quantitative comparison of different interactions in an ionic liquid-nanoparticle hybrid system is hard to assess. Most published reports on nanoparticle stability in ionic liquids have focused on one or two interactions, while few reports have considered a combination of those interactions to maintain nanoparticle stability in ionic liquids. Future research will be beneficial on variables (such as nanoparticle size, temperature, solvent addition and surface modification) affecting each intermolecular interaction, and on the combination of interactions affecting the stability of nanoparticle dispersions in ionic liquids.

Various types of structured ionic liquid and nanoparticle hybrids have been developed in addition to dispersions of nanoparticle in ionic liquids. Colloidal glasses and gels are among the soft materials resulting from nanoparticle dispersion in ionic liquids under different balances of intermolecular interactions. In general, colloidal gels are formed with unstable dispersed nanoparticles interconnecting to a three-dimensional network structure through hydrogen bonding and van der Waals interactions. Colloidal glasses are obtained when the concentrated dispersed nanoparticles cannot aggregate due to strong repulsive interactions, but are rather trapped by neighboring nanoparticles through a cage effect. Colloidal glasses and colloidal gels formed in ionic liquids by polymer-grafted nanoparticles can experience glass-to-gel transition if the polymer solubility in the ionic liquid changes in response to environment changes, which subsequently affects the hydrogen bond and steric repulsion.

Nanoparticles synthesized in situ or dispersed following synthesis can selectively localize into solid-like ordered matrices such as liquid crystals formed by long side-chain ionic liquids or lyotropic liquid crystals formed by amphiphiles in ionic liquids. Nanoparticle-LLC composites are found stable without any precipitation or phase separation. Nanoparticles can locate at ionic liquid-based interfaces as stabilizers in ionic liquid-water/oil emulsions or can be selectively extracted into the one phase, depending on the relative solvophobicities. Besides nanoparticles dispersed in ionic liquids or in ionic liquid-based preformed structures, other types of nanoparticle and ionic liquid hybrids, such as NIMs, can be achieved by ionic liquid chemical bonding with nanoparticles.

Structure formation and nanoparticle localization in nanoparticle-LLC composites in molecular solvents,[192, 208, 209] and on LLC structures formed in ionic liquids have been studied. However, ionic liquid-based nanoparticle-LLC composites are much less studied compared with those in regular solvents. Future research will be beneficial on the structure and corresponding properties and function of ionic liquid-based nanoparticle-LLC composites, and the comparison with those of nanoparticle-LLC composites in molecular solvents with considerations of intermolecular interactions.

Combining novel properties of both nanoparticles and ionic liquids, the unique characteristics of ionic liquid plus nanoparticle hybrids can lead to various applications. On one hand, properties of the nanoparticles, such as thermal stability, catalytic efficiency, adsorption efficiency, and electrical and electrochemical response can be modified and improved through physical/chemical surface modification with ionic liquids.[210] On the other hand, physicochemical and/or electrochemical properties of the ionic liquid and nanoparticle mixture can be better than those of the ionic liquid alone due to interactions within the dispersion.[211] Nanoparticle dispersions in ionic liquids are promising in electrochemical applications due to good proton-transfer ability of ionic liquids and the high electron conductivity afforded by metal nanoparticles or carbon nanotubes. Nanoparticle and ionic liquid hybrids are applied as electrodes or electrolytes in cell batteries, providing better stability and electrical conductivity.[212, 213] Electrochemical sensors have been developed with ionic liquid-nanoparticle composites to achieve rapid responses and high sensitivity and selectivity.[104, 214] Offering the advantage of facile recovery of the catalyst, rationally designed metal nanoparticle/ionic liquid composites have been applied as highly efficient catalysts in multiphase catalytic systems.[104, 215, 216] Reports on applications of ionic liquid and nanoparticle composites have expanded in recent years. Given the promising applications, research on the structure-property relationships of nanoparticle and ionic liquid composite is highly anticipated. Further research on the effects of intermolecular interactions and environmental factors on the phase structure and stability will assist the rational design of novel materials incorporating nanoparticles and ionic liquids.

Acknowledgements: We thank the U.S. National Science Foundation for supporting research in our laboratory in the area of ionic liquids (grants CBET 1033878 and 1159981).

Notes and references

[a] *Department of Chemical and Biological Engineering, University at Buffalo, The State University of New York (SUNY) , Buffalo, New York 14260-4200, USA. Fax: +1-716-645-3822; Tel: +1-716-645-1183; E-mail: palexand@buffalo.edu*

1. J. L. Copeland, *Transport Properties of Ionic Liquids*, Gordon and Breach, 1974.

2. S. Z. El Abedin and F. Endres, *Acc. Chem. Res.*, 2007, **40**, 1106-1113.
3. J. H. Davis, *Chem. Lett.*, 2004, **33**, 1072-1077.
4. K. N. Marsh, J. A. Boxall and R. Lichtenthaler, *Fluid Phase Equilib.*, 2004, **219**, 93-98.
5. P. Walden, *Bull. Acad. Imp. Sci. St.-Petersbourg*, 1914, 405-422.
6. J. S. Wilkes, *Green Chemistry*, 2002, **4**, 73-80.
7. J. Dupont, *Acc. Chem. Res.*, 2011, **44**, 1223-1231.
8. T. L. Greaves and C. J. Drummond, *Chem. Rev.*, 2008, **108**, 206-237.
9. C. A. Angell, N. Byrne and J. P. Belieres, *Acc. Chem. Res.*, 2007, **40**, 1228-1236.
10. G. A. Baker, S. N. Baker, S. Pandey and F. V. Bright, *Analyst*, 2005, **130**, 800-808.
11. T. Ueki and M. Watanabe, *Macromolecules*, 2008, **41**, 3739-3749.
12. M. G. Green, S.; Lee, S.; Firestone, M. A. , *J. Macromol. Sci., Polym. Rev.*, 2009, **49**, 339 - 360
13. H. Weingaertner, *Angew. Chem., Int. Ed.*, 2008, **47**, 654-670.
14. M. Smiglak, A. Metlen and R. D. Rogers, *Acc. Chem. Res.*, 2007, **40**, 1182-1192.
15. T. L. Greaves, D. F. Kennedy, S. T. Mudie and C. J. Drummond, *J. Phys. Chem. B*, 2010, **114**, 10022-10031.
16. M. D. Green and T. E. Long, *J. Macromol. Sci., Polym. Rev.*, 2009, **49**, 291 - 314
17. X. Han and D. W. Armstrong, *Acc. Chem. Res.*, 2007, **40**, 1079-1086.
18. A. E. Visser, R. P. Swatloski, W. M. Reichert, R. Mayton, S. Sheff, A. Wierzbicki, J. H. Davis and R. D. Rogers, *Chem. Commun.*, 2001, 135-136.
19. M. L. Dietz, *Sep. Sci. Technol.*, 2006, **41**, 2047-2063.
20. M. Armand, F. Endres, D. R. MacFarlane, H. Ohno and B. Scrosati, *Nat. Mater.*, 2009, **8**, 621-629.
21. M. C. Buzzeo, R. G. Evans and R. G. Compton, *ChemPhysChem*, 2004, **5**, 1106-1120.
22. S. M. Zakeeruddin and M. Gratzel, *Adv. Funct. Mater.*, 2009, **19**, 2187-2202.
23. W. L. Hough, M. Smiglak, H. Rodriguez, R. P. Swatloski, S. K. Spear, D. T. Daly, J. Pernak, J. E. Grisel, R. D. Carliss, M. D. Soutullo, J. H. Davis and R. D. Rogers, *New J. Chem.*, 2007, **31**, 1429-1436.
24. F. van Rantwijk and R. A. Sheldon, *Chem. Rev.*, 2007, **107**, 2757-2785.
25. M. Moniruzzaman, N. Kamiya and M. Goto, *Org. Biomol. Chem.*, 2010, **8**, 2887-2899.
26. N. V. Plechkova and K. R. Seddon, *Chem. Soc. Rev.*, 2008, **37**, 123-150.
27. A. A. H. Padua, M. F. Gomes and J. N. A. C. Lopes, *Acc. Chem. Res.*, 2007, **40**, 1087-1096.
28. H. F. D. Almeida, A. R. R. Teles, J. A. Lopes-da-Silva, M. G. Freire and J. A. P. Coutinho, *J Chem Thermodyn*, 2012, **54**, 49-54.
29. G. Annat, M. Forsyth and D. R. MacFarlane, *J. Phys. Chem. B*, 2012, **116**, 8251−8258.
30. H. Tokuda, K. Ishii, M. A. B. H. Susan, S. Tsuzuki, K. Hayamizu and M. Watanabe, *J. Phys. Chem. B*, 2006, **110**, 2833-2839.
31. H. Tokuda, K. Hayamizu, K. Ishii, M. A. B. H. Susan and M. Watanabe, *J. Phys. Chem. B*, 2005, **109**, 6103-6110.
32. H. Tokuda, K. Hayamizu, K. Ishii, M. Abu Bin Hasan Susan and M. Watanabe, *J. Phys. Chem. B*, 2004, **108**, 16593-16600.
33. K. Fumino, S. Reimann and R. Ludwig, *Phys. Chem. Chem. Phys.*, 2014, **16**, 21903-21929.
34. D. F. Evans, A. Yamauchi, R. Roman and E. Z. Casassa, *J. Colloid Interface Sci.*, 1982, **88**, 89-96.
35. D. F. Evans, A. Yamauchi, G. J. Wei and V. A. Bloomfield, *J. Phys. Chem.*, 1983, **87**, 3537-3541.
36. R. Ludwig, *Angew. Chem. Int. Ed.*, 2001, **40**, 1808-1827.
37. S. M. Chen, S. J. Zhang, X. M. Liu, J. Q. Wang, J. J. Wang, K. Dong, J. Sun and B. H. Xu, *Phys. Chem. Chem. Phys.*, 2014, **16**, 5893-5906.
38. H. K. Stassen, R. Ludwig, A. Wulf and J. Dupont, *Chemistry - A European Journal*, 2015, **21**, 8324-8335.
39. S. Li, J. L. Banuelos, J. Guo, L. Anovitz, G. Rother, R. W. Shaw, P. C. Hillesheim, S. Dai, G. A. Baker and P. T. Cummings, *J. Phys. Chem. Lett.*, 2012, **3**, 125-130.
40. J. N. A. C. Lopes and A. A. H. Padua, *J. Phys. Chem. B*, 2006, **110**, 3330-3335.
41. K. Dong and S. J. Zhang, *Chem. Eur. J.*, 2012, **18**, 2748-2761.
42. E. W. Castner, J. F. Wishart and H. Shirota, *Acc. Chem. Res.*, 2007, **40**, 1217-1227.
43. O. Russina, A. Triolo, L. Gontrani and R. Caminiti, *J. Phys. Chem. Lett.*, 2012, **3**, 27-33.
44. A. Pinkert, K. N. Marsh, S. S. Pang and M. P. Staiger, *Chem. Rev.*, 2009, **109**, 6712-6728.
45. Y. Cao, J. Wu, J. Zhang, H. Li, Y. Zhang and J. He, *Chem. Eng. J.*, 2009, **147**, 13-21.
46. S. Zhu, Y. Wu, Q. Chen, Z. Yu, C. Wang, S. Jin, Y. Ding and G. Wu, *Green Chem.*, 2006, **8**, 325-327.
47. Z. G. Li, Z. Jia, Y. X. Luan and T. C. Mu, *Curr. Opin. Solid State Mater. Sci.*, 2009, **12**, 1-8.
48. X. C. Duan, J. M. Ma, J. B. Lian and W. J. Zheng, *CrystEngComm*, 2014, **16**, 2550-2559.
49. T. Welton, *Chem. Rev.*, 1999, **99**, 2071-2083.
50. W. S. Miao and T. H. Chan, *Acc. Chem. Res.*, 2006, **39**, 897-908.
51. K. Ueno and M. Watanabe, *Langmuir*, 2011, **27**, 9105-9115.
52. G. S. Fonseca, G. Machado, S. R. Teixeira, G. H. Fecher, J. Morais, M. C. M. Alves and J. Dupont, *J. Colloid Interface Sci.*, 2006, **301**, 193-204.
53. Y. Zhou and M. Antonietti, *J. Am. Chem. Soc.*, 2003, **125**, 14960-14961.
54. Y. Shim and H. J. Kim, *ACS Nano*, 2009, **3**, 1693-1702.
55. T. Fukushima, A. Kosaka, Y. Ishimura, T. Yamamoto, T. Takigawa, N. Ishii and T. Aida, *Science*, 2003, **300**, 2072-2074.
56. H. Zhang and H. Cui, *Langmuir*, 2009, **25**, 2604-2612.
57. D. de Caro, K. Jacob, H. Hahioui, C. Faulmann, L. Valade, T. Kadoya, T. Mori, J. Fraxedasd and L. Viaue, *New J. Chem.*, 2011, **35**, 1315-1319.
58. T. Greaves and C. Drummond, *Chem. Soc. Rev.*, 2013, **42**, 1096-1120.
59. C. Vollmer and C. Janiak, *Coordin. Chem. Rev.*, 2011, **255**, 2039-2057.
60. T. L. Greaves and C. J. Drummond, *Chem. Soc. Rev.*, 2008, **37**, 1709-1726.
61. P. K. Jain, X. H. Huang, I. H. El-Sayed and M. A. El-Sayed, *Acc. Chem. Res.*, 2008, **41**, 1578-1586.
62. P. Alexandridis, *Chem. Eng. Technol.*, 2011, **34**, 15-28.
63. J. Dupont and M. R. Meneghetti, *Curr. Opin. Colloid Interface Sci.*, 2013, **18**, 54-60.
64. W. Zhu and Z. Hou, *Current Inorganic Chemistry*, 2012, **2**, 213-227.
65. D. O. Silva, L. Luza, A. Gual, D. L. Baptista, F. Bernardi, M. J. M. Zapata, J. Morais and J. Dupont, *Nanoscale*, 2014, **6**, 9085-9092.
66. P. Migowski, G. Machado, S. R. Texeira, M. C. M. Alves, J. Morais, A. Traverse and J. Dupont, *Phys. Chem. Chem. Phys.*, 2007, **9**, 4814-4821.
67. H. C. Chang, S. C. Chang, T. C. Hung, J. C. Jiang, J. L. Kuo and S. H. Lin, *J. Phys. Chem. C*, 2011, **115**, 23778-23783.
68. C. W. Scheeren, G. Machado, S. R. Teixeira, J. Morais, J. B. Domingos and J. Dupont, *J. Phys. Chem. B*, 2006, **110**, 13011-13020.
69. M. Zhao, N. Li, L. Zheng, G. Li and L. Yu, *J. Dispersion Sci. Technol.*, 2008, **29**, 1103-1105.
70. H. Wender, L. F. de Oliveira, P. Migowski, A. F. Feil, E. Lissner, M. H. G. Prechtl, S. R. Teixeira and J. Dupont, *J. Phys. Chem. C*, 2010, **114**, 11764-11768.
71. T. Torimoto, K.-i. Okazaki, T. Kiyama, K. Hirahara, N. Tanaka and S. Kuwabata, *Appl. Phys. Lett.*, 2006, **89**, 243117/243111-243117/243113.
72. Y. Hatakeyama, M. Okamoto, T. Torimoto, S. Kuwabata and K. Nishikawa, *J. Phys. Chem. C*, 2009, **113**, 3917-3922.
73. M. T. Kessler, M. K. Hentschel, C. Heinrichs, S. Roitsch and M. H. G. Prechtl, *RSC Advances*, 2014, **4**, 14149-14156.
74. M. Scariot, D. O. Silva, J. D. Scholten, G. Machado, S. R. Teixeira, M. A. Novak, G. Ebeling and J. Dupont, *Angew. Chem., Int. Ed.*, 2008, **47**, 9075-9078.
75. L. Wang, L. Chang, B. Zhao, Z. Yuan, G. Shao and W. Zheng, *Inorg. Chem.* , 2008, **47**, 1443-1452.

76. X. Li, Y. Liu, W. Guo, J. Chen, W. He and F. Peng, *Electrochimica Acta*, 2014, **135**, 550-557.
77. C. Lorbeer, J. Cybinska and A.-V. Mudring, *Journal of Materials Chemistry C: Materials for Optical and Electronic Devices*, 2014, **2**, 1862-1868.
78. A. B. Patil and B. M. Bhanage, *Phys. Chem. Chem. Phys.*, 2014, **16**, 3027-3035.
79. V. Khare, A. Kraupner, A. Mantion, A. Jelicic, A. F. Thuenemann, C. Giordano and A. Taubert, *Langmuir*, 2010, **26**, 10600-10605.
80. C.-H. Liu, B.-H. Mao, J. Gao, S. Zhang, X. Gao, Z. Liu, S.-T. Lee, X.-H. Sun and S.-D. Wang, *Carbon*, 2012, **50**, 3008-3014.
81. Y. Hatakeyama, S. Takahashi and K. Nishikawa, *J. Phys. Chem. C*, 2010, **114**, 11098-11102.
82. T. Kameyama, Y. Ohno, T. Kurimoto, K.-i. Okazaki, T. Uematsu, S. Kuwabata and T. Torimoto, *Phys. Chem. Chem. Phys.*, 2010, **12**, 1804-1811.
83. P. Dash, S. M. Miller and R. W. J. Scott, *Journal of Molecular Catalysis A-Chemical*, 2010, **329**, 86-95.
84. E. Vanecht, K. Binnemans, S. Patskovsky, M. Meunier, J. W. Seo, L. Stappers and J. Fransaer, *Phys. Chem. Chem. Phys.*, 2012, **14**, 5662-5671.
85. D. M. Sabatini, *Leading edge nanotechnology research developments*, Nova Science Publishers, New York, 2007.
86. C. S. S. R. Kumar, Springer, Berlin ; London, 2013.
87. K. Richter, A. Birkner and A. V. Mudring, *Phys. Chem. Chem. Phys.*, 2011, **13**, 7105-7110.
88. K. Ueno, A. Inaba, M. Kondoh and M. Watanabe, *Langmuir*, 2008, **24**, 5253-5259.
89. T. Sakai and P. Alexandridis, *Chem. Mater.*, 2006, **18**, 2577-2583.
90. Q. Li and A. Li, *Asian Journal of Chemistry*, 2012, **24**, 847-850.
91. E. Zapp, D. Brondani, I. C. Vieira, J. Dupont and C. W. Scheeren, *Electroanalysis*, 2011, **23**, 1124-1133.
92. B. G. Wang, X. B. Wang, W. J. Lou and J. C. Hao, *J. Colloid Interface Sci.*, 2011, **362**, 5-14.
93. J. M. Obliosca, I. H. J. Arellano, M. H. Huang and S. D. Arco, *Mater. Lett.*, 2010, **64**, 1109-1112.
94. L. L. Lazarus, A. S. J. Yang, S. Chu, R. L. Brutchey and N. Malmstadt, *Lab Chip*, 2010, **10**, 3377-3379.
95. V. Khare, Z. Li, A. Mantion, A. A. Ayi, S. Sonkaria, A. Voelkl, A. F. Thuenemann and A. Taubert, *J. Mater. Chem.*, 2010, **20**, 1332-1339.
96. T. Singh and A. Kumar, *J. Phys. Chem. B*, 2008, **112**, 12968-12972.
97. S. Aparicio, M. Atilhan and F. Karadas, *Ind. Eng. Chem. Res.*, 2010, **49**, 9580-9595.
98. S. Kuwabata, A. Kongkanand, D. Oyamatsu and T. Torimoto, *Chemistry Letters*, 2006, **35**, 600-601.
99. K. Lunstroot, L. Baeten, P. Nockemann, J. Martens, P. Verlooy, X. Ye, C. Gorller-Walrand, K. Binnemans and K. Driesen, *J. Phys. Chem. C*, 2009, **113**, 13532-13538.
100. L. Rodriguez-Arco, M. T. Lopez-Lopez, J. D. G. Duran, A. Zubarev and D. Chirikov, *J. Phys.: Condens. Matter*, 2011, **23**, 455101.
101. Q. Li, U. Jonas, X. S. Zhao and M. Kappl, *Asia-Pacific Journal of Chemical Engineering*, 2008, **3**, 255-268.
102. T. Tadros, *Colloids and Interface Science Series*, 2007, **1**, 1-22.
103. C. R. O'Melia, *Interface Science and Technology*, 2006, **10**, 317-362.
104. J. Dupont and J. D. Scholten, *Chem. Soc. Rev.*, 2010, **39**, 1780-1804.
105. A. Podgorsek, A. Pensado, C. Santini, M. Gomes and A. Padua, *J. Phys. Chem. C*, 2013, **117**, 3537-3547.
106. A. I. Frolov, K. Kirchner, T. Kirchner and M. V. Fedorov, *Faraday Discuss*, 2012, **154**, 235-247.
107. J. C. Rubim, F. A. Trindade, M. A. Gelesky, R. F. Aroca and J. Dupont, *J. Phys. Chem. C*, 2008, **112**, 19670-19675.
108. H. S. Schrekker, M. A. Gelesky, M. P. Stracke, C. M. L. Schrekker, G. Machado, S. R. Teixeira, J. C. Rubim and J. Dupont, *J. Colloid Interface Sci.*, 2007, **316**, 189-195.
109. O. P. Khatri, K. Adachi, K. Murase, K.-i. Okazaki, T. Torimoto, N. Tanaka, S. Kuwabata and H. Sugimura, *Langmuir*, 2008, **24**, 7785-7792.
110. B. W. Ninham, *Adv. Colloid Interface Sci.* , 1999, **83**, 1-17.
111. S. L. Carnie and D. Y. C. Chan, *J. Colloid Interf. Sci.*, 1993, **161**, 260-264.
112. D. F. Evans and H. Wennerström, *The colloidal domain: Where physics, chemistry, biology, and technology meet*, 2nd edn., Wiley-VCH, New York, 1999.
113. J. N. Israelachvili, *Intermolecular and Surface Forces*, Third Edition edn., Academic Press, 2011.
114. C. Daguenet, P. J. Dyson, I. Krossing, A. Oleinikova, J. Slattery, C. Wakai and H. Weingartner, *J. Phys. Chem. B*, 2006, **110**, 12682-12688.
115. A. Kumar, *J. Solution Chem.* , 2008, **37**, 203-214.
116. T. Matsuda, Y. Mishima, S. Azizian, H. Matsubara, T. Takiue and M. Aratono, *Colloid Polym. Sci.*, 2007, **285**, 1601-1605.
117. J. Dong, D. S. Corti, E. I. Franses, Y. Zhao, H. T. Ng and E. Hanson, *Langmuir*, 2010, **26**, 6995-7006.
118. D. Guo, G. X. Xie and J. B. Luo, *J. Phys. D: Appl. Phys.*, 2014, **47**, 013001.
119. C. J. van Oss, *Interfacial forces in aqueous media*, 2nd edn., Taylor & Francis, Boca Raton, Fla., 2006.
120. D. Grasso, K. Subramaniam, M. Butkus, K. Strevett and J. Bergendahl, *Rev. Environ. Sci. Biotechnol.*, 2002, **1**, 17-38.
121. M. Iida, S. Kawakami, E. Syouno, H. Er and E. Taguchi, *J. Colloid Interface Sci.*, 2011, **356**, 630-638.
122. Y. Liang, N. Hilal, P. Langston and V. Starov, *Advances in Colloid and Interface Science*, 2007, **134-135**, 151-166.
123. D. S. Frost, M. Machas and L. L. Dai, *Langmuir*, 2012, **28**, 13924-13932.
124. R. Atkin and G. G. Warr, *J. Phys. Chem. C*, 2007, **111**, 5162-5168.
125. E. Redel, M. Walter, R. Thomann, C. Vollmer, L. Hussein, H. Scherer, M. Krueger and C. Janiak, *Chem. Eur. J.*, 2009, **15**, 10047-10059.
126. M. Mamusa, J. Sirieix-Plenet, F. Cousin, R. Perzynski, E. Dubois and V. Peyre, *J. Phys.: Condens. Matter*, 2014, **26**, 284113.
127. M. Mamusa, J. Siriex-Plenet, F. Cousin, E. Dubois and V. Peyre, *Soft Matter*, 2014, **10**, 1097-1101.
128. A. Wittmar, D. Ruiz-Abad and M. Ulbricht, *J. Nanopart. Res.*, 2012, **14**, 651/651-651/610.
129. A. Wittmar and M. Ulbricht, *Ind. Eng. Chem. Res.*, 2012, **51**, 8425-8433.
130. A. Wittmar, D. Gautam, C. Schilling, U. Doerfler, W. Mayer-Zaika, M. Winterer and M. Ulbricht, *J. Nanopart. Res.*, 2014, **16**, 1-14.
131. B. Sarkar, V. Venugopal, M. Tsianou and P. Alexandridis, *Colloids and Surfaces A: Physicochem. Eng. Aspects*, 2013, **422**, 155-164.
132. R. Evans and D. H. Napper, *J. Colloid Interface Sci.*, 1977, **58**, 390-407.
133. Y. N. Lin, T. W. Smith and P. Alexandridis, *J. Colloid Interf. Sci.*, 2002, **255**, 1-9.
134. P. F. Luckham, *Advances in Colloid and Interface Science*, 1991, **34**, 191-215.
135. M. J. Rosen and J. T. Kunjappu, *Surfactants and Interfacial Phenomena*, Wiley, 2012.
136. Y. N. Lin and P. Alexandridis, *J. Phys. Chem. B*, 2002, **106**, 10834-10844.
137. O. Russina and A. Triolo, *Faraday Discuss*, 2012, **154**, 97-109.
138. C. Oumahi, J. Lombard, S. Casale, C. Calers, L. Delannoy, C. Louis and X. Carrier, *Catal. Today*, 2014, **235**, 58-71.
139. I. Choi, H. Ahn and M. J. Park, *Macromolecules*, 2011, **44**, 7327-7334.
140. K. Ueno, T. Fukai, T. Nagatsuka, T. Yasuda and M. Watanabe, *Langmuir*, 2014, **30**, 3228-3235.
141. K. Ueno, A. Inaba, T. Ueki, M. Kondoh and M. Watanabe, *Langmuir*, 2010, **26**, 18031-18038.
142. K. Swiderski, A. McLean, C. M. Gordon and D. H. Vaughan, *Chem. Commun.*, 2004, 2178-2179.
143. S. H. Lee and S. B. Lee, *Chem. Commun.*, 2005, 3469-3471.
144. F. C. C. Oliveira, L. M. Rossi, R. F. Jardim and J. C. Rubim, *J. Phys. Chem. C*, 2009, **113**, 8566-8572.
145. N. Jain, X. L. Zhang, B. S. Hawkett and G. G. Warr, *ACS Appl. Mater. Inter.*, 2011, **3**, 662-667.
146. H. C. Chang, T. C. Hung, S. C. Chang, J. C. Jiang and S. H. Lin, *J. Phys. Chem. C*, 2011, **115**, 11962-11967.
147. E. Antoniou and P. Alexandridis, *European Polymer Journal*, 2010, **46**, 324-335.

148.E. Arunan, G. R. Desiraju, R. A. Klein, J. Sadlej, S. Scheiner, I. Alkorta, D. C. Clary, R. H. Crabtree, J. J. Dannenberg, P. Hobza, H. G. Kjaergaard, A. C. Legon, B. Mennucci and D. J. Nesbitt, *Pure Appl. Chem.*, 2011, **83**, 1619-1636.

149.A. A. Oliferenko, P. V. Oliferenko, J. G. Huddleston, R. D. Rogers, V. A. Palyulin, N. S. Zefirov and A. R. Katritzky, *J. Chem. Inf. Comput. Sci.*, 2004, **44**, 1042-1055.

150.C. Reichardt, *Chem. Rev.*, 1994, **94**, 2319-2358.

151.K. Tamura, N. Nakamura and H. Ohno, *Biotechnol. Bioeng.*, 2012, **109**, 729-735.

152.P. A. Hunt, *Mol. Simul.*, 2006, **32**, 1-10.

153.R. C. Dougherty, *J. Chem. Phys.*, 1998, **109**, 7372-7378.

154.M. Meot-Ner and L. W. Sieck, *J. Am. Chem. Soc.*, 1983, **105**, 2956-2961.

155.K. A. Fletcher and S. Pandey, *Appl. Spectrosc.*, 2002, **56**, 266-271.

156.K. R. Seddon, A. Stark and M. J. Torres, *Pure Appl. Chem.*, 2000, **72**, 2275-2287.

157.M. J. Earle and K. R. Seddon, *Pure Appl. Chem.*, 2000, **72**, 1391-1398.

158.Q. G. Zhang, N. N. Wang, S. L. Wang and Z. W. Yu, *J. Phys. Chem. B*, 2011, **115**, 11127-11136.

159.M. G. Freire, L. M. N. B. F. Santos, A. M. Fernandes, J. A. P. Coutinho and I. M. Marrucho, *Fluid Phase Equilib.*, 2007, **261**, 449-454.

160.T. Takamuku, Y. Kyoshoin, T. Shimomura, S. Kittaka and T. Yamaguchi, *J. Phys. Chem. B*, 2009, **113**, 10817-10824.

161.C. D. Tran, S. H. D. Lacerda and D. Oliveira, *Appl. Spectrosc.*, 2003, **57**, 152-157.

162.N. Winterton, *J. Mater. Chem.*, 2006, **16**, 4281-4293.

163.M. G. Freire, C. M. S. S. Neves, P. J. Carvalho, R. L. Gardas, A. M. Fernandes, I. M. Marrucho, L. M. N. B. F. Santos and J. A. P. Coutinho, *J. Phys. Chem. B*, 2007, **111**, 13082-13089.

164.N. D. Khupse and A. Kumar, *J. Solution Chem.*, 2009, **38**, 589-600.

165.M. Moreno, F. Castiglione, A. Mele, C. Pasqui and G. Raos, *J. Phys. Chem. B*, 2008, **112**, 7826-7836.

166.L. A. S. Ries, F. A. do Amaral, K. Matos, E. M. A. Martini, M. O. de Souza and R. F. de Souza, *Polyhedron*, 2008, **27**, 3287-3293.

167.M. Lopez-Pastor, M. J. Ayora-Canada, M. Valcarcel and B. Lendl, *J. Phys. Chem. B*, 2006, **110**, 10896-10902.

168.J. A. Smith, O. Werzer, G. B. Webber, G. G. Warr and R. Atkin, *J. Phys. Chem. Lett.*, 2010, **1**, 64-68.

169.I. Szilagyi, T. Szabo, A. Desert, G. Trefalt, T. Oncsik and M. Borkovec, *Phys. Chem. Chem. Phys.*, 2014, **16**, 9515-9524.

170.W. Jiang, Y. Wang and G. A. Voth, *J. Phys. Chem. B*, 2007, **111**, 4812-4818.

171.A. Mele, C. D. Tran and S. H. D. Lacerda, *Angew. Chem. Int. Ed.*, 2003, **42**, 4364-4366.

172.H. C. Chang, J. C. Jiang, Y. C. Liou, C. H. Hung, T. Y. Lai and S. H. Lin, *J. Chem. Phys.*, 2008, **129**, 044506.

173.J. Luczak, J. Hupka, J. Thoming and C. Jungnickel, *Colloids Surf., A*, 2008, **329**, 125-133.

174.J. Bowers, C. P. Butts, P. J. Martin, M. C. Vergara-Gutierrez and R. K. Heenan, *Langmuir*, 2004, **20**, 2191-2198.

175.T. Singh and A. Kumar, *J. Phys. Chem. B*, 2007, **111**, 7843-7851.

176.T. L. Greaves, D. F. Kennedy, A. Weerawardena, N. M. K. Tse, N. Kirby and C. J. Drummond, *J. Phys. Chem. B*, 2011, **115**, 2055-2066.

177.D. S. Frost and L. L. Dai, *Langmuir*, 2011, **27**, 11339-11346.

178.J. R. Stokes and W. J. Frith, *Soft Matter*, 2008, **4**, 1133-1140.

179.J. Le Bideau, L. Viau and A. Vioux, *Chem. Soc. Rev.*, 2011, **40**, 907-925.

180.S. Wang, B. Hsia, C. Carraro and R. Maboudian, *Journal of Materials Chemistry A: Materials for Energy and Sustainability*, 2014, **2**, 7997-8002.

181.C.-L. Park, A. Y. Jee, M. Lee and S.-g. Lee, *Chem. Commun.* , 2009, 5576-5578.

182.S. S. Moganty, S. Srivastava, Y. Y. Lu, J. L. Schaefer, S. A. Rizvi and L. A. Archer, *Chem. Mater.*, 2012, **24**, 1386-1392.

183.K. Ueno, K. Hata, T. Katakabe, M. Kondoh and M. Watanabe, *J. Phys. Chem. B*, 2008, **112**, 9013-9019.

184.N. Li, S. H. Zhang, L. Q. Zheng, B. Dong, X. W. Li and L. Yu, *Phys. Chem. Chem. Phys.*, 2008, **10**, 4375-4377.

185.I. Goodchild, L. Collier, S. L. Millar, I. Prokes, J. C. D. Lord, C. P. Butts, J. Bowers, J. R. P. Webster and R. K. Heenan, *J. Colloid Interface Sci.*, 2007, **307**, 455-468.

186.J. Larionova, Y. Guari, C. Blanc, P. Dieudonne, A. Tokarev and C. Guerin, *Langmuir*, 2009, **25**, 1138-1147.

187.M. W. Zhao, Y. N. Gao and L. Q. Zheng, *Colloids Surf., A*, 2010, **369**, 95-100.

188.G. D. Zhang, X. Chen, Y. R. Zhao, F. M. Ma, B. Jing and H. Y. Qiu, *J. Phys. Chem. B*, 2008, **112**, 6578-6584.

189.P. Alexandridis and A. Tsoutsoura, *PMSE Preprints*, 2011, **105**, 1077-1078.

190.T. Dai, L. Ge and R. Guo, *J. Mater. Res.*, 2009, **24**, 333-341.

191.J. Huh, V. V. Ginzburg and A. C. Balazs, *Macromolecules*, 2000, **33**, 8085-8096.

192.B. Sarkar and P. Alexandridis, *Langmuir*, 2012, **28**, 15975-15986.

193.R. B. Thompson, V. V. Ginzburg, M. W. Matsen and A. C. Balazs, *Science*, 2001, **292**, 2469-2472.

194.A. Tsoutsoura and P. Alexandridis, *PMSE Preprints*, 2010, **102**, 168-169.

195.P. Alexandridis, D. L. Zhou and A. Khan, *Langmuir*, 1996, **12**, 2690-2700.

196.D. S. Frost, E. M. Nofen and L. L. Dai, *Advances in Colloid and Interface Science*, 2014, **206**, 92-105.

197.A. Wang, L. Chen, F. Xu and Z. Yan, *RSC Advances*, 2014, **4**, 45251–45257.

198.B. P. Binks, A. K. F. Dyab and P. D. I. Fletcher, *Chem. Commun.*, 2003, 2540-2541.

199.Y. Liu, G. Wu, H. Fu, Z. Jiang, S. Chen and M. Sha, *Dalton Trans.*, 2010, **39**, 3190-3194.

200.S. Chakraborty, K. Jaehnichen, H. Komber, A. A. Basfar and B. Voit, *Macromolecules*, 2014, **47**, 4186-4198.

201.G. Zhou, Z. Luo and X. Fu, *Journal of Agricultural and Food Chemistry*, 2014, **62**, 8214-8220.

202.A. Serra, E. Gomez, J. F. Lopez-Barbera, J. Nogues and E. Valles, *ACS Nano*, 2014, **8**, 4630-4639.

203.H. Sawada, S. Kodama, K. Tsunashima and M. Sugiya, *J. Mater. Sci.*, 2007, **42**, 2532-2535.

204.T. Fukushima and T. Aida, *Chem. Eur. J.*, 2007, **13**, 5048-5058.

205.R. Rodriguez, R. Herrera, A. B. Bourlinos, R. P. Li, A. Amassian, L. A. Archer and E. P. Giannelis, *Appl. Organomet. Chem.*, 2010, **24**, 581-589.

206.N. J. Fernandes, T. J. Wallin, R. A. Vaia, H. Koerner and E. P. Giannelis, *Chem. Mater.*, 2014, **26**, 84-96.

207.M. L. Jespersen, P. A. Mirau, E. von Meerwall, R. A. Vaia, R. Rodriguez and E. P. Giannelis, *ACS Nano*, 2010, **4**, 3735-3742.

208.B. Sarkar, E. Ayandele, V. Venugopal and P. Alexandridis, *Macromolecular Chemistry and Physics*, 2013, **214**, 2716-2724.

209.B. Sarkar and P. Alexandridis, *Prog. Polym. Sci.*, 2015, **40**, 33-62.

210.B. Xin and J. Hao, *Chem. Soc. Rev.*, 2014, **43**, 7171-7187.

211.M.-A. Neouze, M. Kronstein and F. Tielens, *Chem. Commun.* , 2014, **50**, 10929-10936.

212.F.-L. Chen, I. W. Sun, H. P. Wang and C. H. Huang, *J. Nanomater.*, 2009, **2009**, 472950/472951-472950/472954

213.C. Neo and J. Ouyang, *Electrochim. Acta*, 2012, **85**, 1-8.

214.S. Xu, Y. Lu, H. Wang, H. Abruna and L. Archer, *Journal of Materials Chemistry A: Materials for Energy and Sustainability*, 2014, **2**, 17723-17729.

215.J. D. Scholten, B. C. Leal and J. Dupont, *ACS Catal.*, 2012, **2**, 184-200.

216.A. V. Perdikaki, O. C. Vangeli, G. N. Karanikolos, K. L. Stefanopoulos, K. G. Beltsios, P. Alexandridis, N. K. Kanellopoulos and G. E. Romanos, *J. Phys. Chem. C*, 2012, **116**, 16398-16411.